Models of segregation in soft-particle suspensions and re-entrant rheology in surfactant solutions

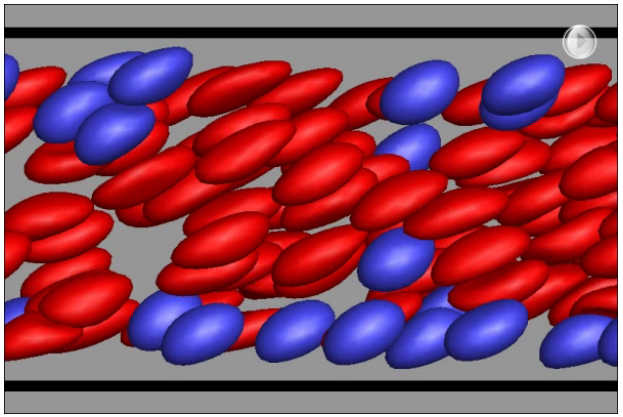

Michael D. Graham

Department of Chemical & Biological Engineering

University of Wisconsin-Madison

Blood flow in the microcirculation

- "Cell-free" layer
- "Margination" of white blood cells and platelets
- Plasma-skimming results in lower hematocrit in side-braches

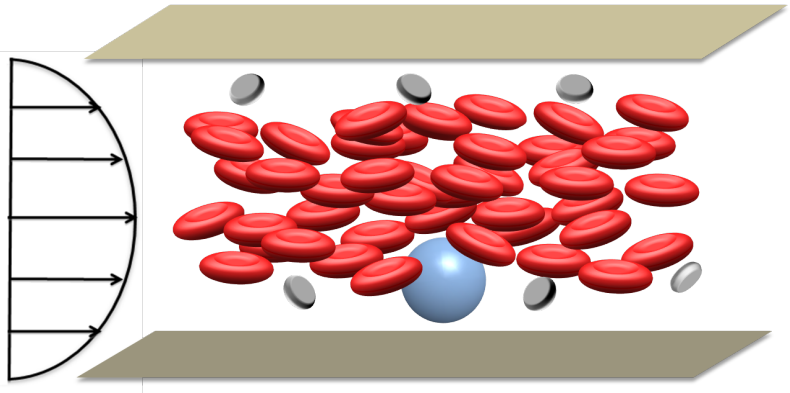

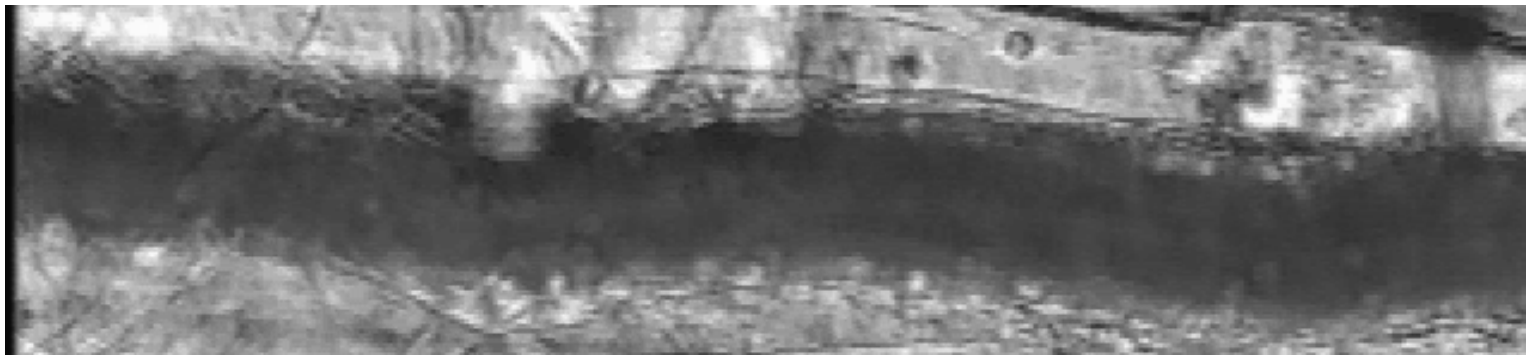

Leukocyte rolling in rat cremaster muscle
(Courtesy Ingrid Sarelius, U. Rochester)

Size and deformability of formed elements in blood

- "Real-time deformability cytometry": high-throughput screen of whole blood. (Otto et al., TU-Dresden)

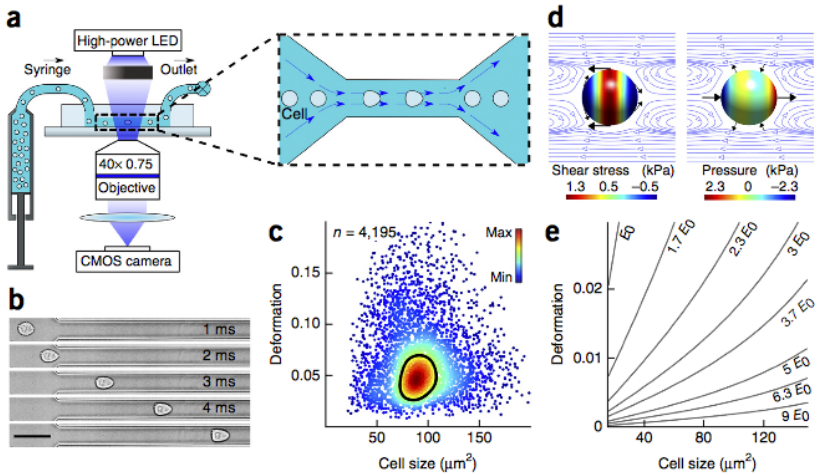

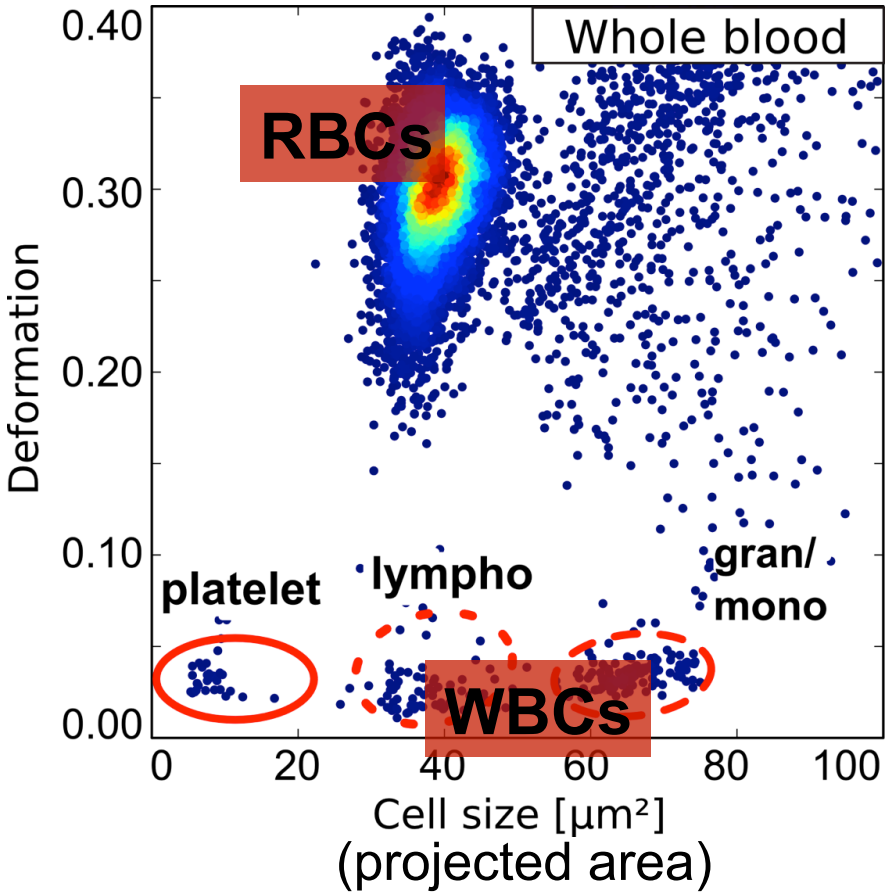

(Otto et al., Nature Methods 2015)

Related/prior studies of margination

- Computational studies: Gompper/Winkler, Aidun/Neitzel, Freund, Bagchi, Shaqfeh, Fogelson, Krüger, Karniadakis/ Caswell, Gekle…
  - mostly focused on realistic treatment of blood: details for one parameter set, not trends as parameters vary

Theory/mechanism

- Eckstein: phenomenological drift-diffusion equation
- Fogelson: extracting drift-diffusion parameters from simulations
- Shaqfeh: statistics of velocity fluctuations, master equation model for cell-free layer

Aims and approaches

- Aims
  - What factors (size, rigidity, shape…) affect migration and margination phenomena?
  - What mechanisms underlie these phenomena?
- Approaches
  - Direct simulations of idealized model cells/particles in confined flow:
    - Suspensions, single particle and pair collision studies
    - Effects of stiffness and size contrast
  - Reduced models that capture essential mechanisms
  - Experimental corroboration in blood

Binary suspensions: simulation

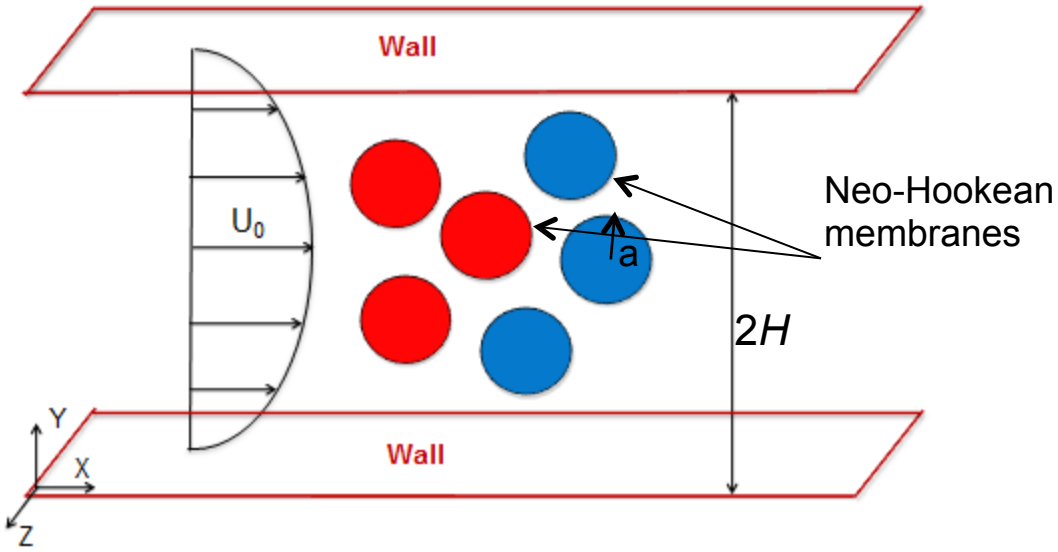

Capillary Number $\dfrac{\mu \dot{\gamma}_w a}{G}$

Stiff Particle: G ↑ ↔ Ca ↓

Flexible Particle: G ↓ ↔ Ca ↑

Reynolds Number $\dfrac{\rho \dot{\gamma}_w H^2}{\mu} << 1$

Number fraction of particles X_f & X_s

($X_f + X_s = 1$)

Viscosity ratio $\lambda = 1$

Volume fraction ϕ

Confinement ratio $C = H / 2a$

Binary suspension in Couette flow, dilute in stiff

Red: Flexible Blue: Stiff

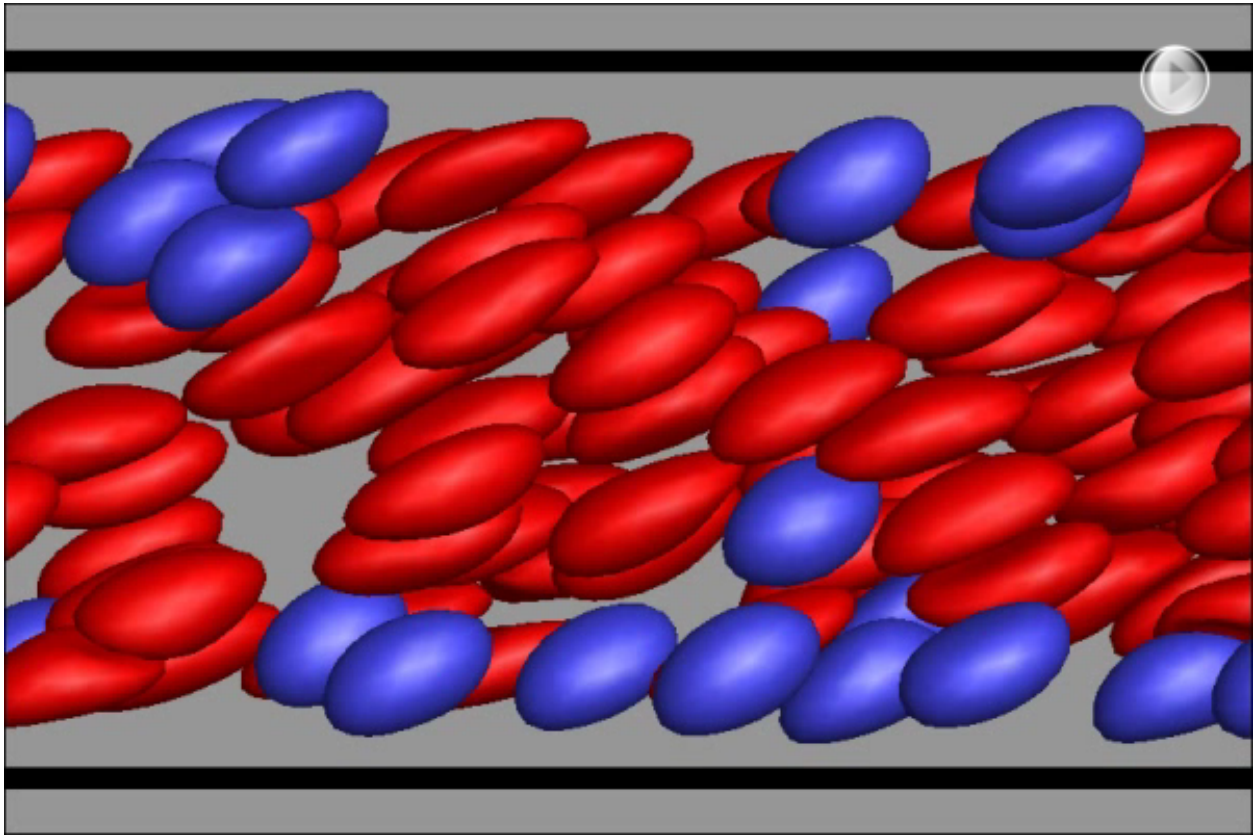

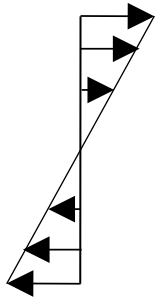

$Ca_s = 0.2$
$Ca_f = 0.5$
$\Phi = 0.2$
$C = 5.08$
$X_f = 0.8$

Stiff particles accumulate in the near wall region: margination
→ Substantial segregation can occur due only to stiffness contrast

Kumar & G., PRE 2011

Binary suspension in Couette flow, dilute in floppy

Red: Floppy Blue: Stiff

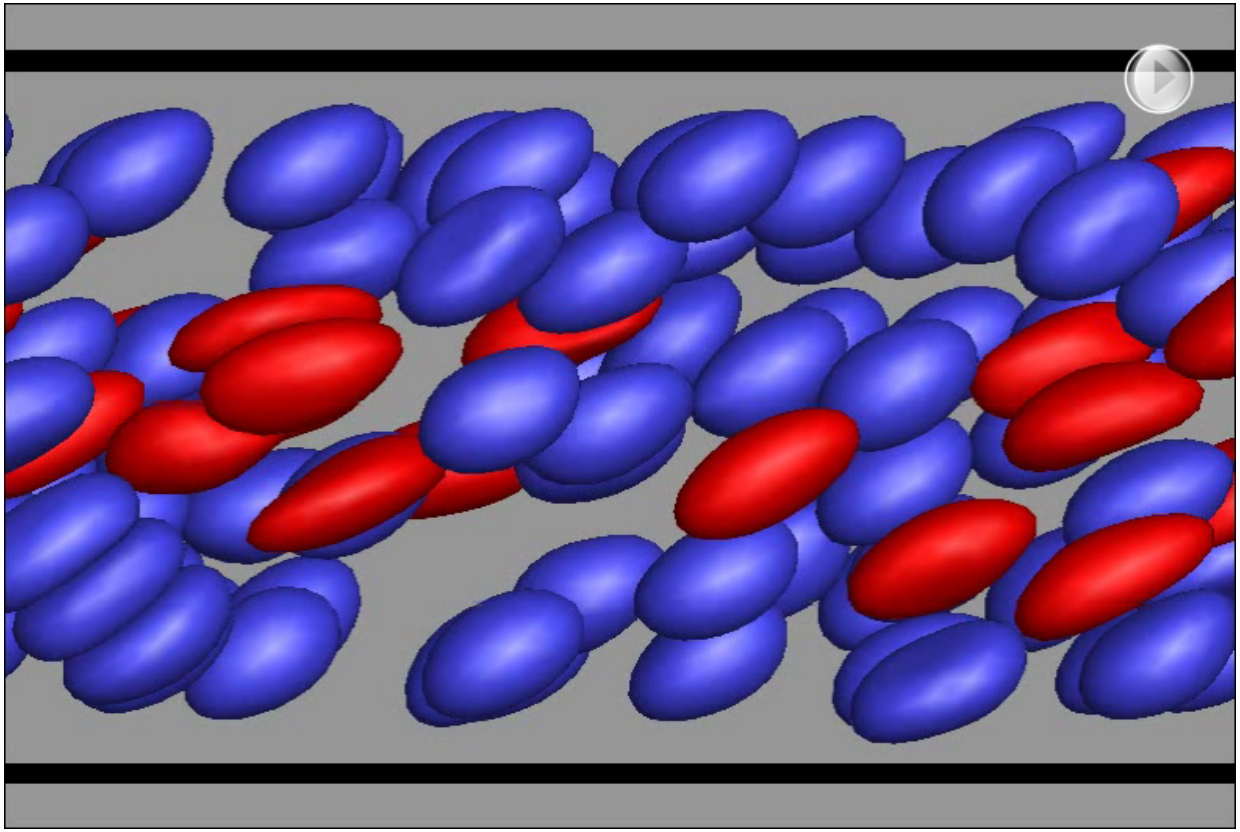

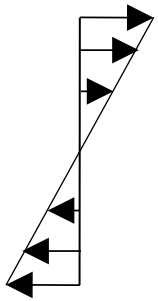

$Ca_s = 0.2$
$Ca_f = 0.5$
$\Phi = 0.2$
$C = 5.08$
$X_f = 0.2$

Flexible particles accumulate around the centerline: “demargination”

Binary suspension of large and small particles

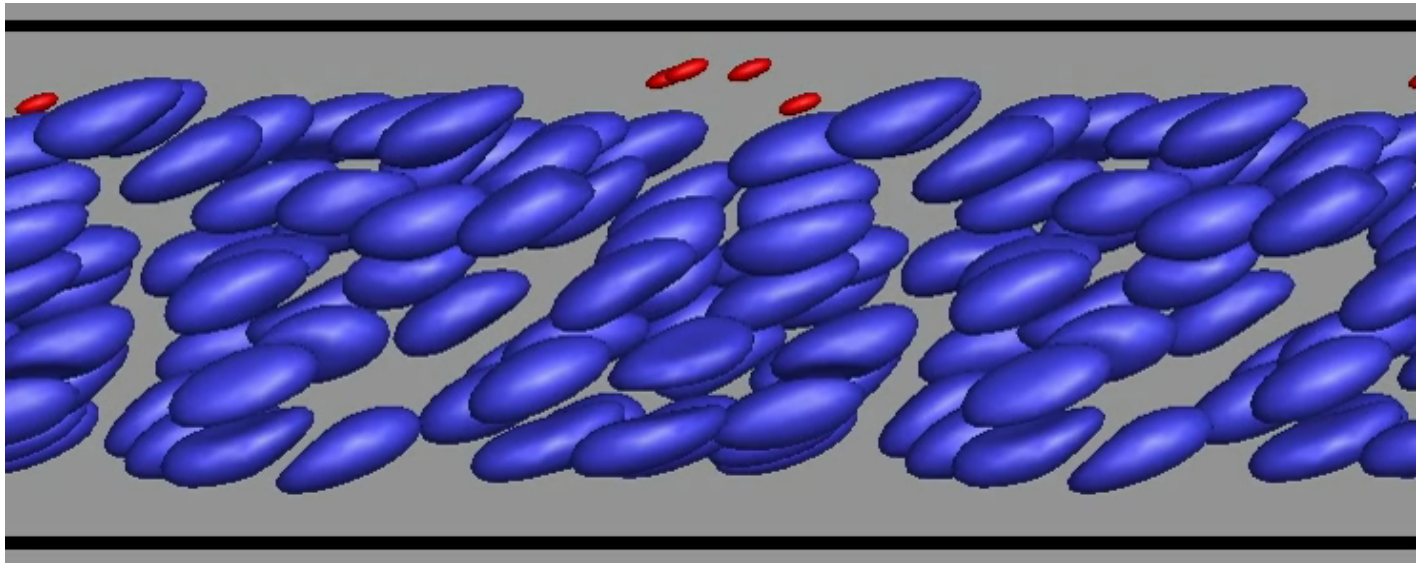

size ratio: $S = 0.3$
confinement ratio: $C = 5.08$
$X_s = 0.1$
$\varphi = 0.16$
$Ca_s = Ca_b = 0.5$

Small particles marginate

Kumar, Henriquez & G. J Fluid Mech., 2014

Key processes in suspension transport

Cross-Stream displacement in pair collisions → shear-induced diffusion

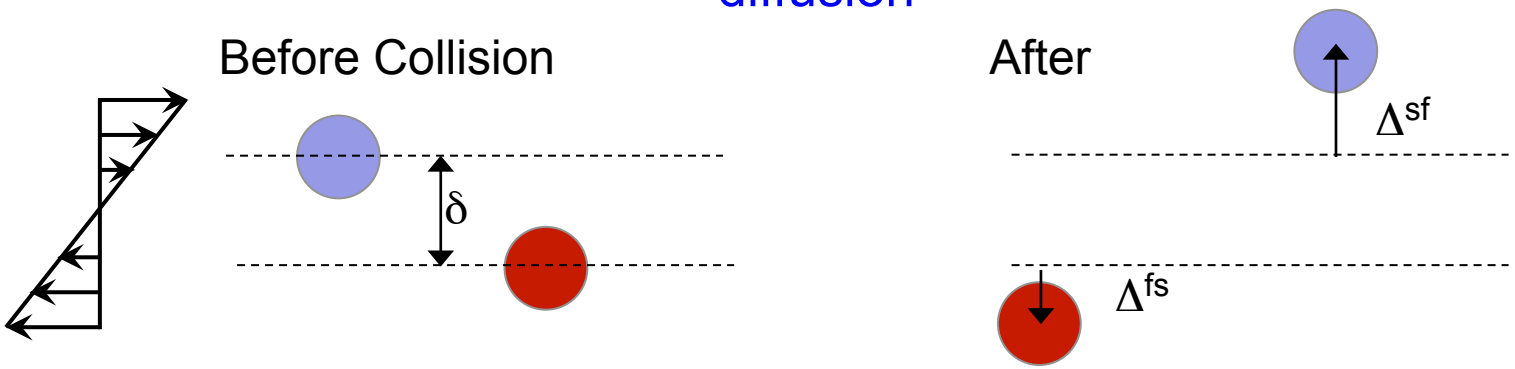

Wall-induced migration

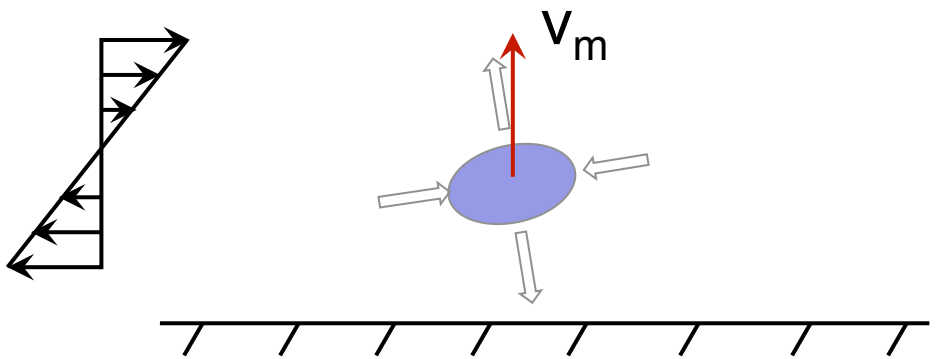

Leighton and Acrivos JFM 1987
Smart and Leighton, Phys. Fluids 1991

Cross-stream displacements in pair collisions

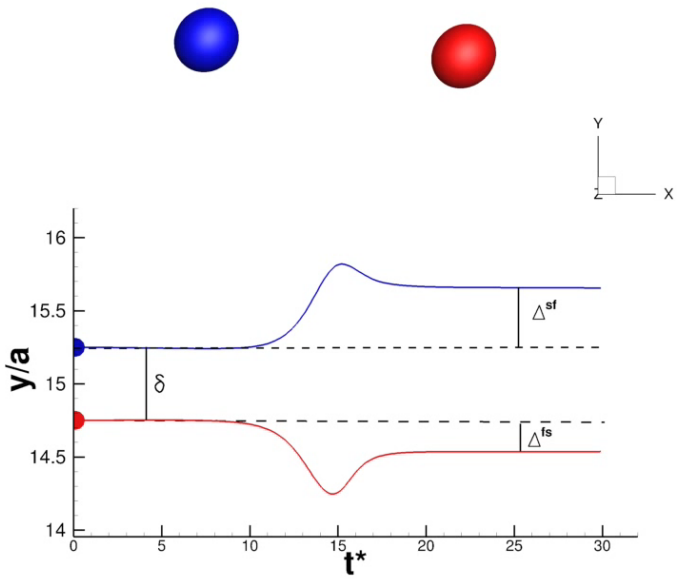

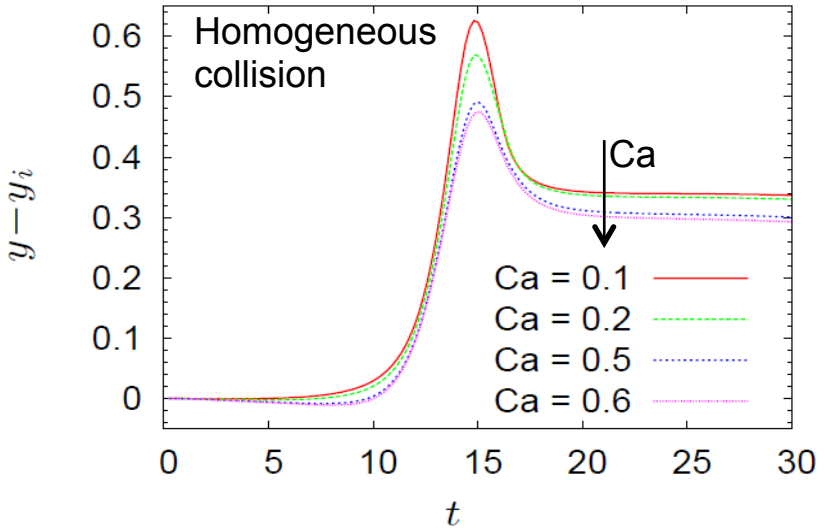

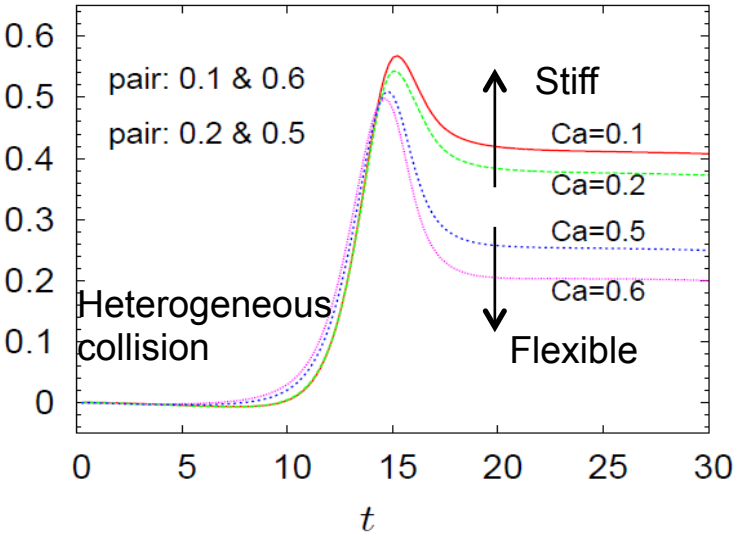

- Cross-stream displacement is a weak function of Ca
- Stiff particles undergo larger cross-stream displacement
- Similar results occur for heterogeneity in size and shape
  - Small particles displace more (at same Ca)
  - Oblate (i.e. RBC-like) particles displace less at same equatorial radius

Kumar & G. PRE 2011, Sinha & G. 2016

Pair collisions and migration velocity

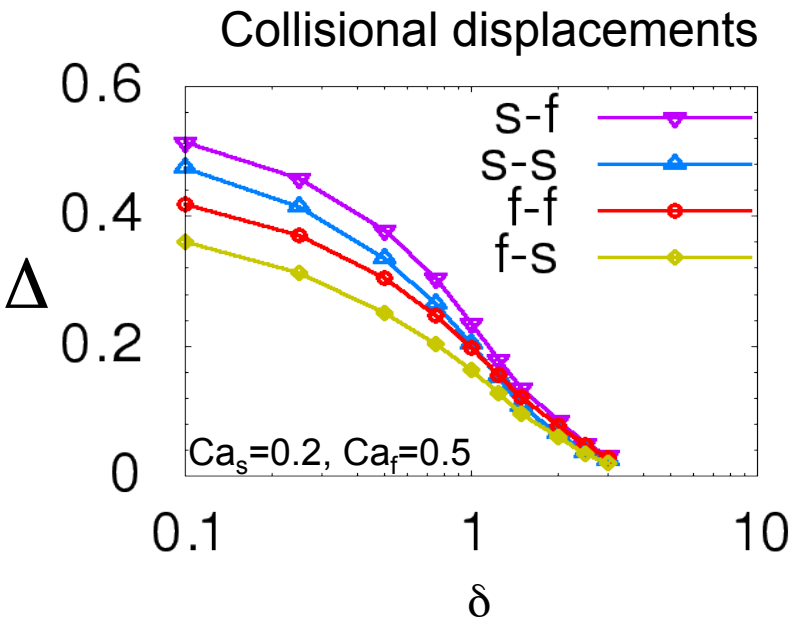

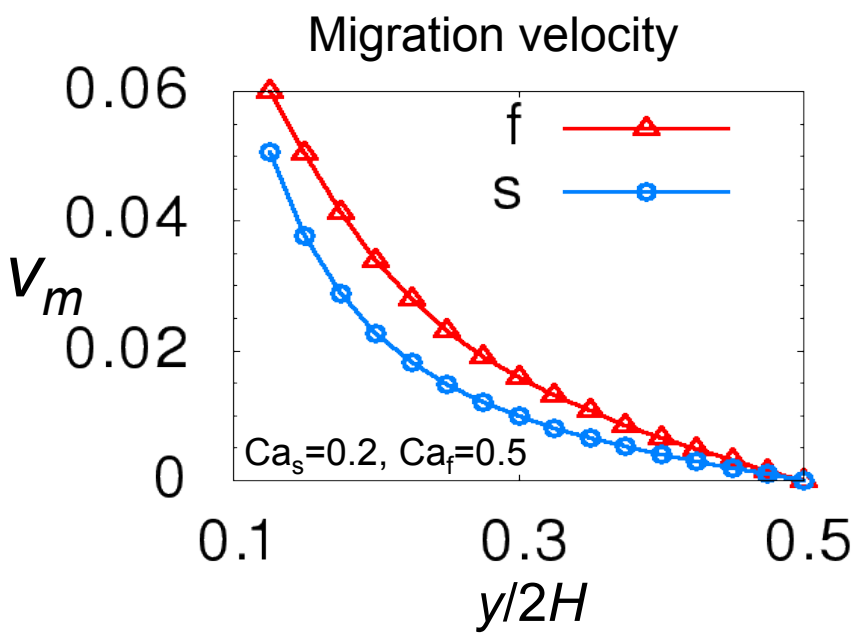

Stiff and flexible (δ<1):

$$\Delta^{fs} < \Delta^{ff} < \Delta^{ss} < \Delta^{sf}$$

Big and little:

$$\Delta^{bl} < \Delta^{ll} < \Delta^{bb} < \Delta^{lb}$$

$$v_m = a\dot{\gamma} f_m(\mathrm{Ca}, \mathrm{shape}) \frac{a^2}{y^2}$$

small<big
stiff<flexible

Master equation: migration and pair collisions

cf. Zurita-Gotor et al. 2012, Narsimhan & Shaqfeh 2013, Qi & Shaqfeh 2017

migration

$$\frac{\partial n_\alpha(y,t)}{\partial t} = -\frac{\partial}{\partial y}\left(v_{\alpha m}(y) n_\alpha(y,t)\right)$$

$$+ \sum_{\beta=1}^{N_s} \left(\int_{-(2H-y)}^{y} \int_{-\infty}^{\infty} \left\{ n_\alpha(y-\Delta_y^{\alpha\beta}, z-\Delta_z^{\alpha\beta}, t) \right.\right.$$

$$\times n_\beta(y-\Delta_y^{\alpha\beta}-\delta_y, z-\Delta_z^{\alpha\beta}-\delta_z, t)$$

$$\left.\left. - n_\alpha(y,z,t) n_\beta(y-\delta_y, z-\delta_z, t) \right\} v_{rel}(y,\delta_y)\, d\delta_z d\delta_y \right)$$

pair collisions

- Numerical solutions are possible using deterministic (Shaqfeh) or stochastic methods (Blawzdziewicz, Kumar and G.)
- Simplifications are also possible…

Kumar & G. PRL 2012, JFM 2014

Nonlinear/nonlocal drift-diffusion equation

Expand master equation for small Δ:

$$\frac{\partial n_\alpha}{\partial t} = -\frac{\partial}{\partial y}\left(v_d^\alpha n_\alpha - \frac{\partial}{\partial y}(D_\alpha n_\alpha)\right)$$

$$v_d^\alpha(y) = v_m^\alpha(y) - \sum_{\beta=1}^{N_s}\int_{-r_{cut}}^{r_{cut}} n_\beta(y-\delta)\,\Delta^{\alpha\beta}(\delta)\,\dot{\gamma}|\delta|\,d\delta,$$

nonlocal

$$D_\alpha(y) = \frac{1}{2}\sum_{\beta=1}^{N_s}\int_{-r_{cut}}^{r_{cut}} n_\beta(y-\delta)\,\{\Delta^{\alpha\beta}(\delta)\}^2\,\dot{\gamma}|\delta|\,d\delta.$$

Steady state (solve self-consistently):

$$n_\alpha(y) = n_\alpha(y_0)\,\frac{D_\alpha(y_0)}{D_\alpha(y)}\,e^{\int_{y_0}^{y} -v_d^\alpha(y)/D_\alpha(y)\,dy}$$

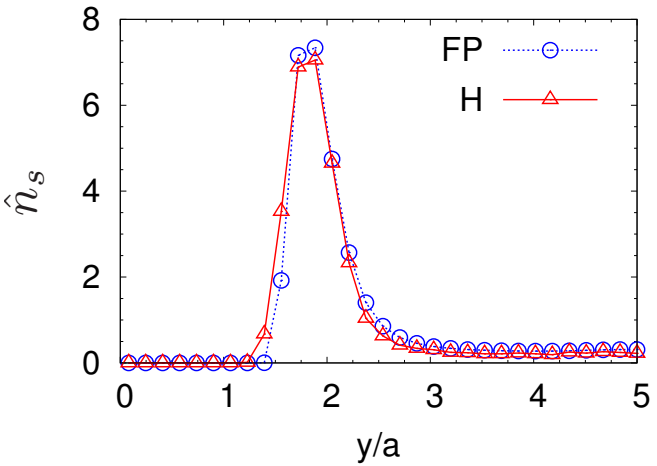

(a) stiff

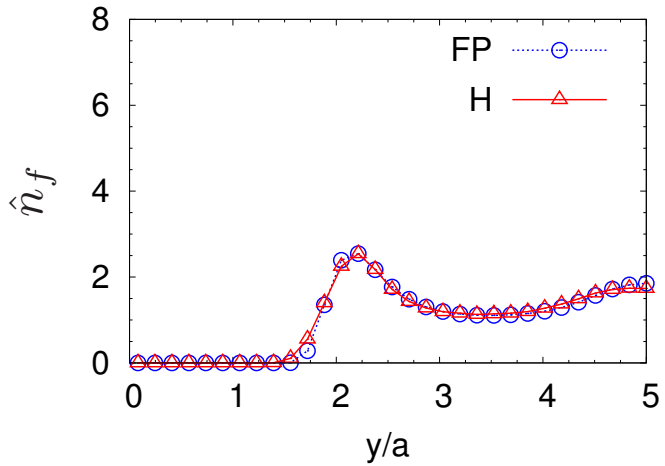

(b) floppy

X_f=0.99
φ=0.12

- Good agreement with stochastic simulations of master equation
- Near-wall peak in primary ← nonlocal dependence of v_d and D on n

Kumar, Henriquez & G. JFM 2014

Simplified drift-diffusion model

- Derived from master equation
- Binary suspension
- Primary (p) and trace (t) components: $\alpha = p$ or t
- Collisions dominated by primary – trace component is passive
- Local approximations in collision integral

$$\frac{\partial n_\alpha}{\partial t} = -\frac{\partial}{\partial y}\left(v_{\alpha d} n_\alpha - \frac{\partial}{\partial y}(D_\alpha n_\alpha)\right)$$

$$v_{\alpha d}(y) = v_{\alpha m}(y) + v_{\alpha c}(y)$$

Migration | Collisional drift | Shear-induced (collisional) diffusion

Primary: $v_{pm} = K_{pm}\left(\frac{1}{y^2} - \frac{1}{(2C-y)^2}\right)$ $\quad v_{pc} = -K_{pc}\frac{\partial n_p \dot{\gamma}}{\partial y}$ $\quad D_p = K_{pd} n_p \dot{\gamma}$

Trace: $v_{tm} = K_{tm}\left(\frac{1}{y^2} - \frac{1}{(2C-y)^2}\right)$ $\quad v_{tc} = -K_{tc}\frac{\partial n_p \dot{\gamma}}{\partial y}$ $\quad D_t = K_{td} n_p \dot{\gamma}$

By symmetry, collisional drift only arises from gradients

Henriquez, Sinha and G., PRL 2015

Simplified drift-diffusion model: details

Start with 3D model. Assume homogeneity in z:

$$\widehat{\Delta_y^{\alpha p}}(\delta_y) = \int_{-r_{cut}}^{r_{cut}} \Delta_y^{\alpha p}(\delta_y, \delta_z) d\delta_z,$$

$$\widehat{\left(\Delta_y^{\alpha p}\right)^2}(\delta_y) = \int_{-\infty}^{\infty} \{\Delta_y^{\alpha p}(\delta_y, \delta_z)\}^2 d\delta_z.$$

Collision integrals:

$$K_{\alpha c} = 2 \int_0^{r_{cut}} \widehat{\Delta_y^{\alpha p}}(\delta_y) \delta_y^2 \, d\delta_y \quad *$$

$$K_{\alpha d} = \int_0^{r_{cut}} \widehat{\left(\Delta_y^{\alpha p}\right)^2}(\delta_y) \delta_y \, d\delta_y$$

* $\widehat{\Delta_y^{\alpha p}}(\delta_y) \sim \delta_y^{-2}$. For convergence we need a cutoff due to confinement or influence of a third particle.

Simplified drift-diffusion model: simple shear

Steady solution:

$$\phi_p = \begin{cases} 0, & y < l_d \\ \phi_{pc}\left(1 - \frac{2\eta_p}{C\phi_{pc}}\frac{(C-y)^2}{y(2C-y)}\right), & y > l_d \end{cases} \qquad \eta_p = \frac{\kappa_{pm}}{\kappa_{pc} + 2\kappa_{pd}}$$

$$\phi_t = \begin{cases} 0, & y < l_d \\ \phi_{tc}\left(\frac{\phi_p(y)}{\phi_{pc}}\right)^{M}, & y > l_d \end{cases} \qquad l_d = C\left(1 - \sqrt{\frac{C\phi_{pc}}{2\eta_p + C\phi_{pc}}}\right)$$

$$M = \frac{\kappa_{pc} + 2\kappa_{pd}}{\kappa_{td}}\left(\frac{\kappa_{tm}}{\kappa_{pm}} - \frac{\kappa_{tc} + \kappa_{td}}{\kappa_{pc} + 2\kappa_{pd}}\right)$$

migration ratio

collisional transport ratio

A discriminant for margination!

Margination regimes:

- M > 1: demargination
- 0 < M < 1: weak margination
  - no peak in profile
- -1 < M < 0: moderate margination
  - peak at edge of depletion layer
- Blowup (no steady solution) when M < -1
  - Strong margination
  - all of trace component eventually drains into marginal layer
  - strong prediction

Binary suspensions:

- M changes with rigidity ratio
- M changes with size ratio

Analytically solvable model that captures key mechanisms and features of margination

Master curve for cell-free layer thickness

Relation between CFL thickness and average volume fraction can be written:

$$\frac{\bar{\phi} C}{\eta_p} = 2\frac{C}{l_d}\frac{(1-\frac{l_d}{C})}{(2-\frac{l_d}{C})} - \ln\left(2\frac{C}{l_d} - 1\right)$$

$$= f\left(\frac{l_d}{C}\right)$$

This implies that with only one adjustable parameter η_p all CFL thickness data should fall onto a single **master curve**…
(This works better than it should – captures tube flow results too)

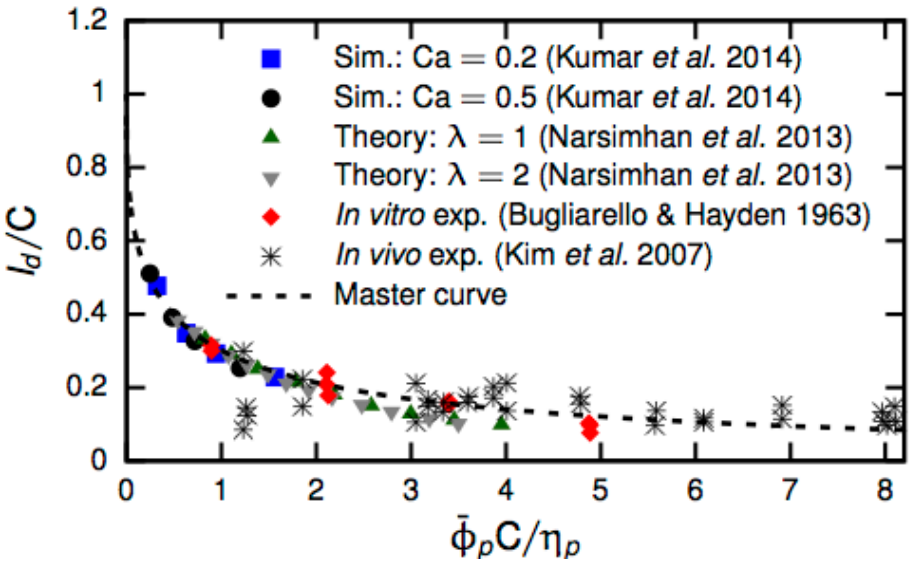

CFL thickness from direct simulations, nonlocal kinetic theory, *in vitro* and *in vivo* experiments, and the master curve. In all cases $0.136 < \eta_p < 0.85$

Theory captures dependence of cell-free layer thickness on confinement and concentration

Margination regimes, M > -1

Number density profiles

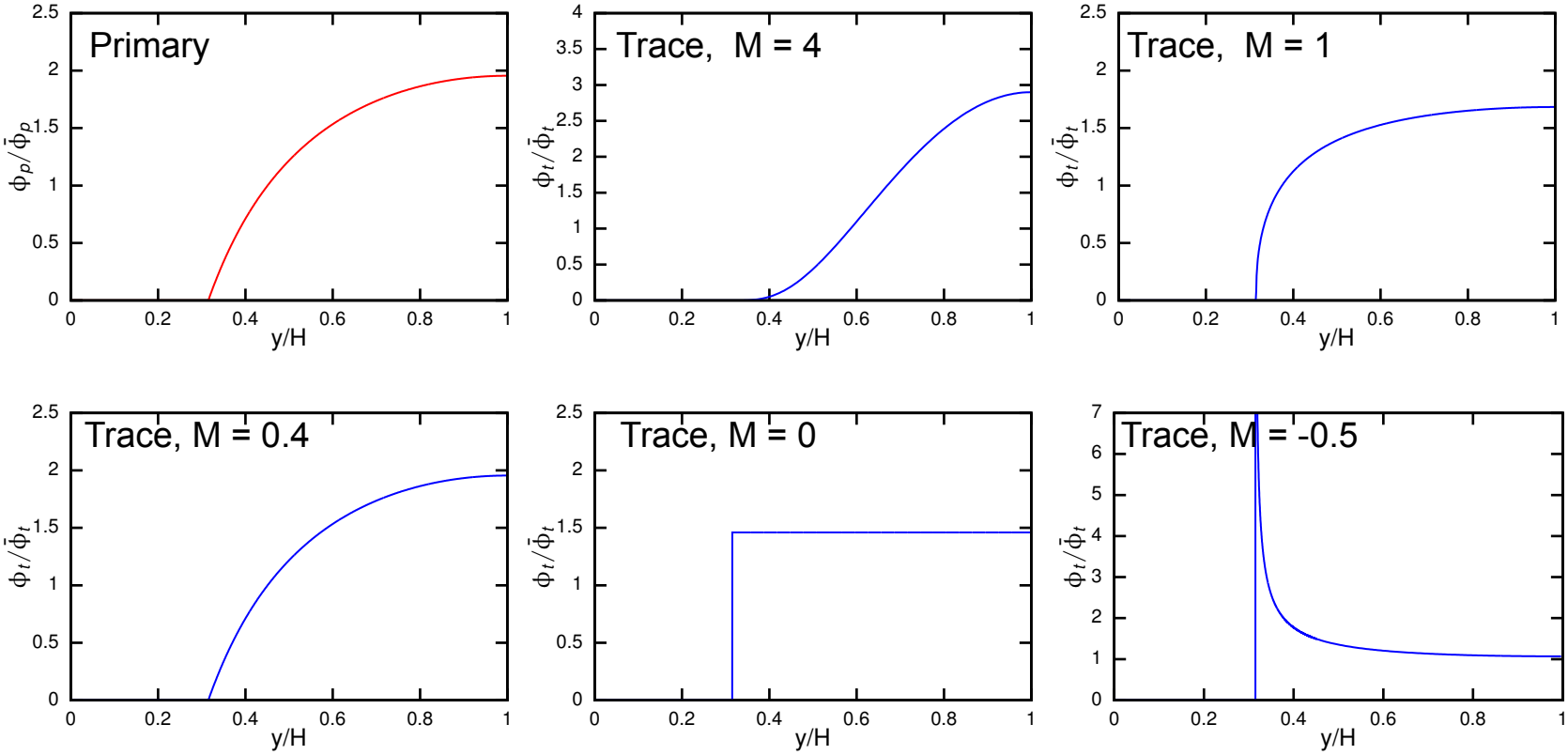

Demargination → margination as M decreases
Simplified model fails to capture near-wall peak in primary component

“Drainage transition”, M < -1

Centerline concentration vs. M

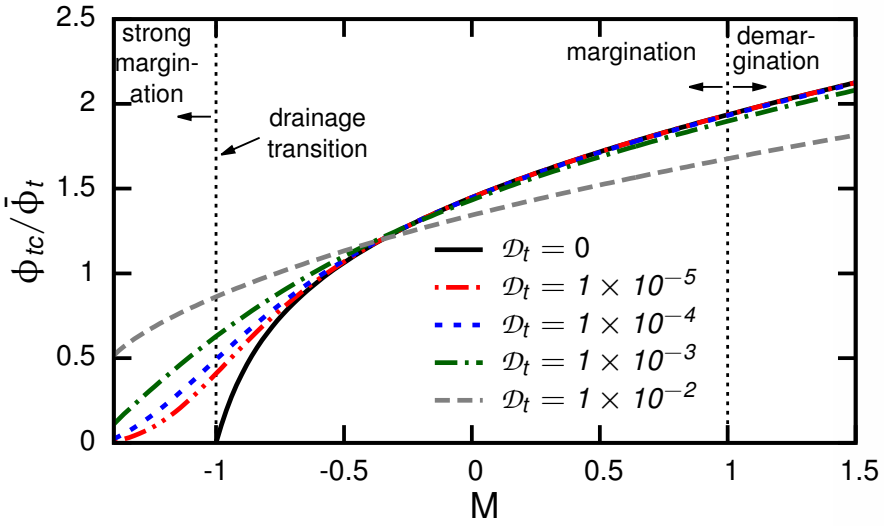

Time dependence

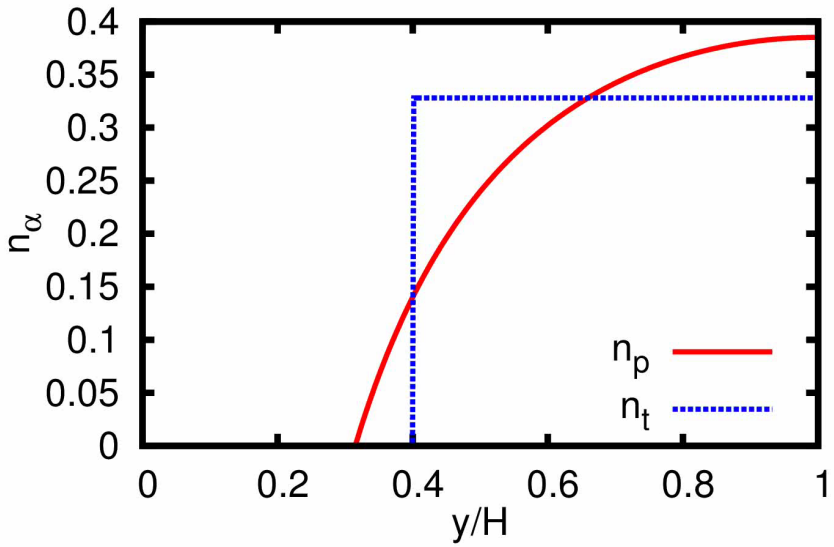

- For M < -1, trace component is completely removed from bulk: “drainage transition”
- For a rigid trace particle with deformable primary component M is always < -1
- Diffusion regularizes this but sharp change near M=-1 remains

- Trace component evolves toward singular solution – spike
- Regularized by trace-trace collisions (infinitely dilute approx. fails)

Drainage transition in simulations

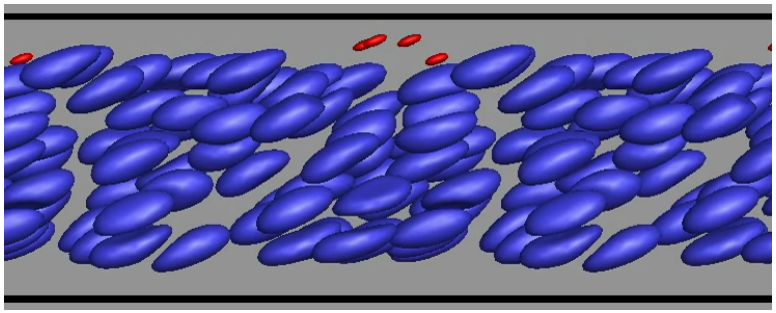

$$S = \frac{a_t}{a_p} \text{ @ fixed Ca}$$

$$F = \frac{G_p}{G_t} = \frac{\mathrm{Ca}_t}{\mathrm{Ca}_p}$$

Centerline concentration vs. S or F

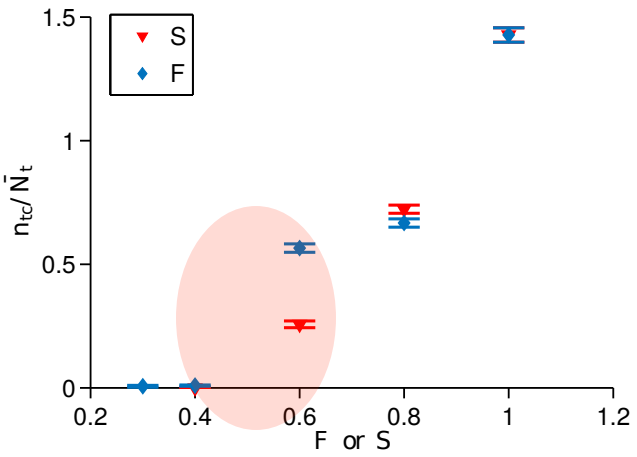

Distribution of small in large

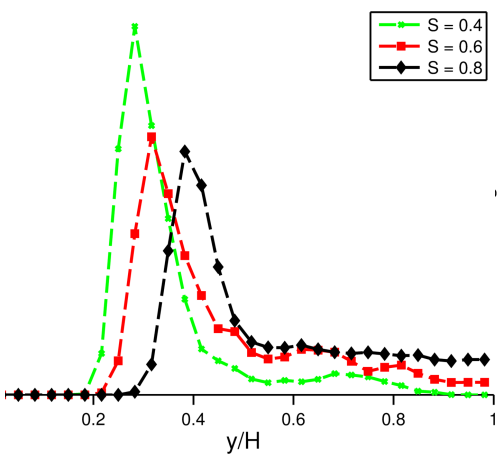

Distribution of stiff in flexible

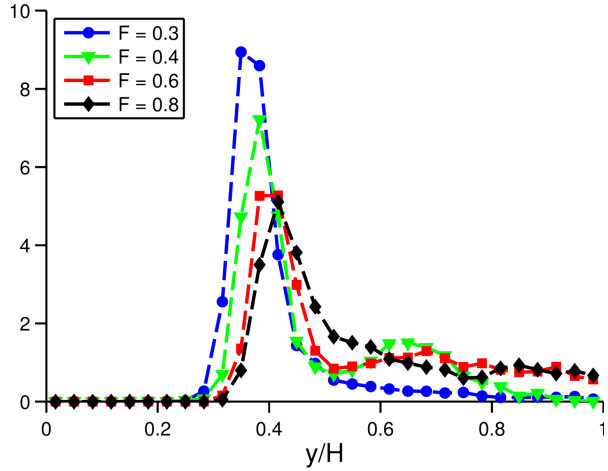

Drainage transition occurs with decreasing ratio of flexibility or size

Poiseuille flow: kinetic theory model

$r_{cut} < 2|C - y|$ – far from center:

$$\frac{\partial \phi_\alpha}{\partial t} = -\frac{\partial}{\partial y}\left\{ v_{\alpha m}\phi_\alpha - \left[\frac{\partial}{\partial y}\left(\phi_p \dot{\gamma}\right) - \frac{f}{2}\phi_p \frac{d\dot{\gamma}}{dy}\right]\phi_\alpha \left(2\int_0^{r_{cut}} \delta|\delta|\Delta d\delta\right) \right.$$
$$\left. -\frac{\partial}{\partial y}\left(\phi_\alpha \phi_p \dot{\gamma}\right)\left(\int_0^{r_{cut}} |\delta|\Delta^2 d\delta\right)\right\}$$

Shear rate vanishes:
Need to keep h.o.t.

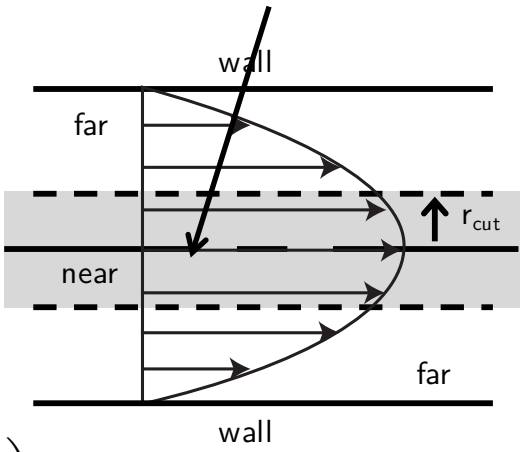

$r_{cut} > 2|C - y|$ – near center:

$$\frac{\partial \phi_\alpha}{\partial t} = -\frac{\partial}{\partial y}\left\{ v_{\alpha m}\phi_\alpha - \left[\frac{\partial}{\partial y}\left(\phi_p \dot{\gamma}\right) - \frac{f}{2}\phi_p \frac{d\dot{\gamma}}{dy}\right]\phi_\alpha \left(2\int_0^{2|C-y|} \delta|\delta|\Delta d\delta\right) \right.$$
$$-\frac{\partial}{\partial y}\left(\phi_\alpha \phi_p \dot{\gamma}\right)\left(\int_0^{2|C-y|} |\delta|\Delta^2 d\delta\right) + \frac{1}{2}\phi_\alpha \frac{\partial \phi_p}{\partial y}\frac{d\dot{\gamma}}{dy}\left(2\int_{2|C-y|}^{r_{cut}} \delta^3 \Delta d\delta\right)$$
$$\left. +\frac{1}{2}\frac{\partial}{\partial y}\left(\phi_\alpha \phi_p\right)\frac{d\dot{\gamma}}{dy}\left(\int_{2|C-y|}^{r_{cut}} \delta^2 \Delta^2 d\delta\right) + \phi_\alpha \phi_p \dot{\gamma}\left(2\int_{2|C-y|}^{r_{cut}} \delta \Delta d\delta\right)\right\}$$

$$f = \begin{cases} 1, & \text{if } y < C \\ 3, & \text{if } y > C \end{cases}$$

Keep approximate versions of terms that don't vanish on centerline

Poiseuille flow: kinetic theory model

migration

$$\frac{\partial \phi_\alpha}{\partial t} = -\frac{\partial}{\partial y}\left\{ v_{\alpha m}\phi_\alpha - \kappa_{\alpha c}\left[\frac{\partial}{\partial y}\left(\phi_p\left(1-\frac{y}{C}\right)\right) + \frac{f}{2C}\phi_p\right]\phi_\alpha \right.$$

collisional drift

$$-\kappa_{\alpha d}\frac{\partial}{\partial y}\left(\phi_\alpha\phi_p\left(1-\frac{y}{C}\right)\right)$$

shear-induced diffusion

$$\left. -\kappa'_{\alpha c}\frac{1}{2C}\phi_\alpha\frac{\partial \phi_p}{\partial y} - \kappa'_{\alpha d}\frac{1}{2C}\frac{\partial}{\partial y}\left(\phi_\alpha\phi_p\right)\right\}$$

New terms due to centerline

$$\dot{\gamma}(y) = \left(1-\frac{y}{C}\right) \qquad \frac{d\dot{\gamma}}{dy} = -\frac{1}{C}$$

- Drift-diffusion model for Poiseuille flow
- Centerline terms required to prevent blowup
  cf. Miller & Morris, JNNFM 2006

Poiseuille flow: effect of confinement

Concentration profiles, C = 5.08

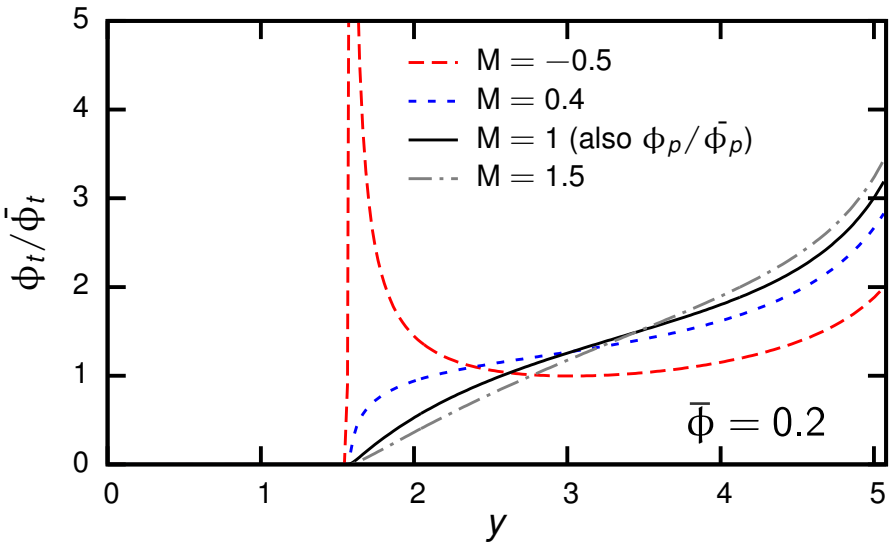

Concentration profiles, C = 20

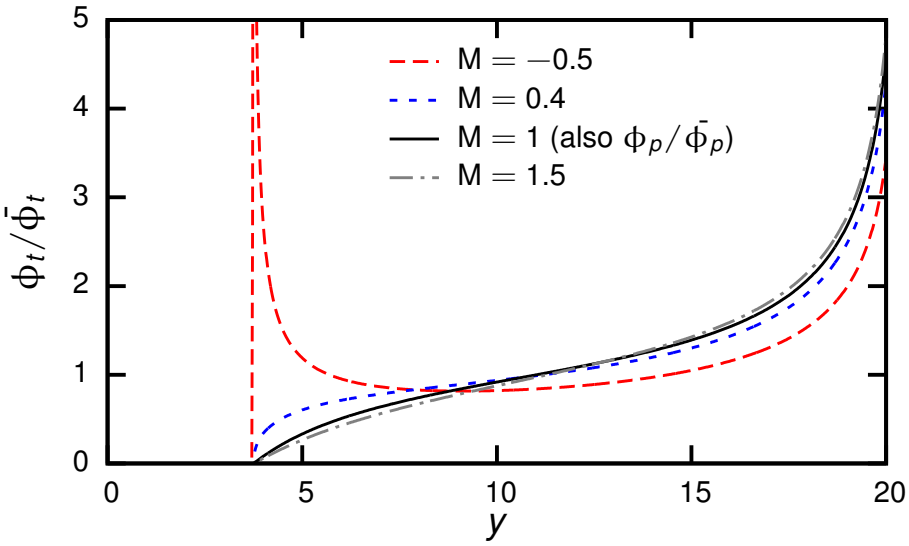

As C increases:

- Depletion layer thickens (agrees with theory)
- Centerline peak increases

Poiseuille flow: drainage transition

Concentration profiles

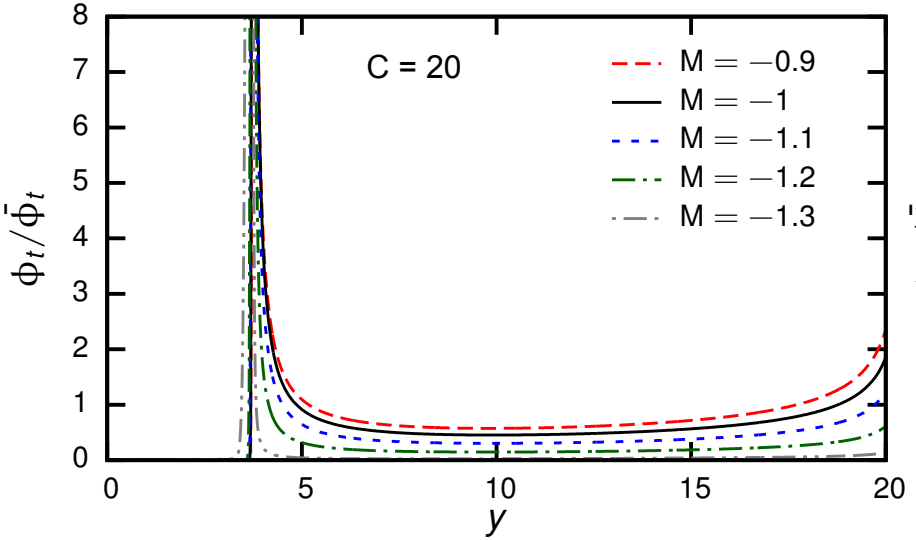

Centerline conc. *vs.* M

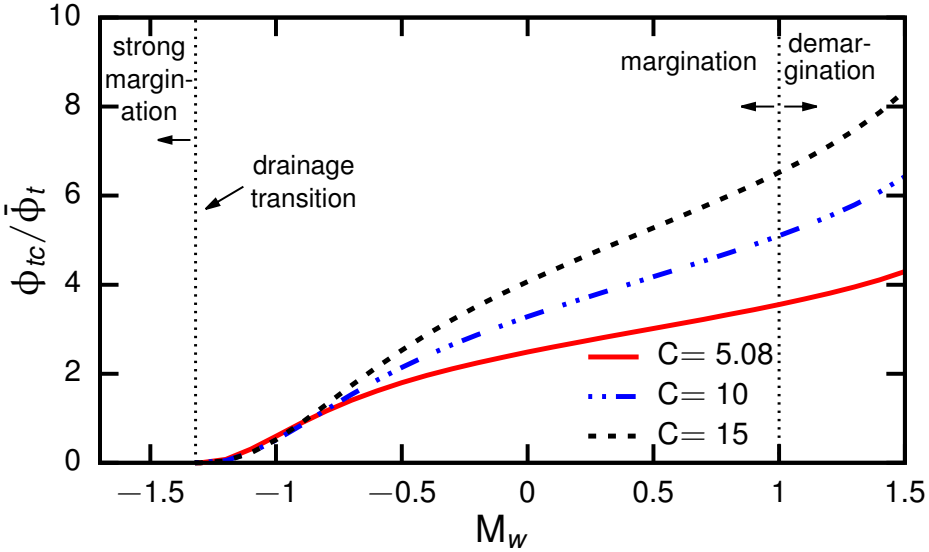

$\bar{\phi} = 0.2$

- Complete drainage of the bulk is again observed for M sufficiently negative

Poiseuille flow: simulation results

Results for segregation by stiffness contrast

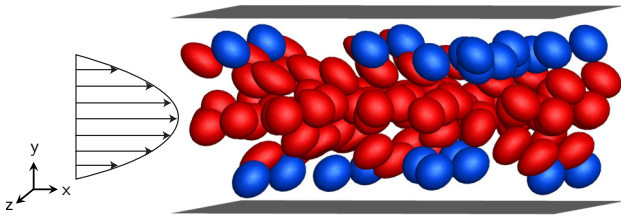

$t = 1788$, F = 0.2

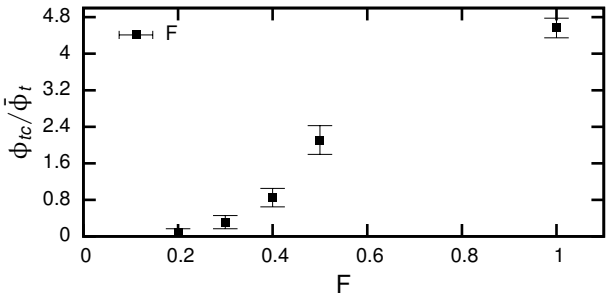

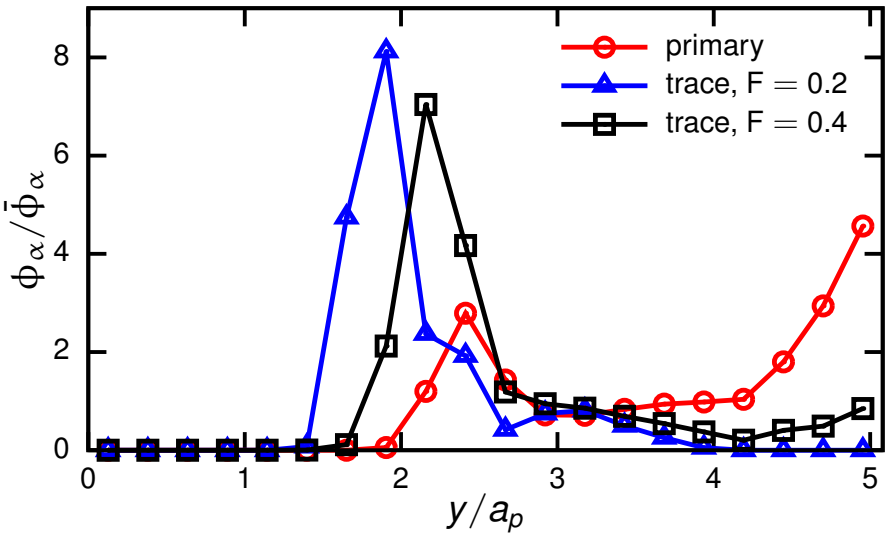

- Centerline peak in primary – also a smaller peak near wall (nonlocal theory is required to capture this)
- Centerline peak in trace for F above drainage transition (predicted by model)
- Drainage transition appears

Conclusions

- Segregation can occur by rigidity or size alone:
  - In suspensions of primarily flexible/large particles, the stiff/small particles marginate
  - In suspensions of primarily stiff/small particles, flexible/large particles *demargin*ate

- Model based on collisions and migration:
  - Qualitatively reproduces detailed results
  - Yields analytical discriminant for margination regimes based on migration and collisional displacement ratios
  - Yields expression for cell-free layer thickness that fits simulation and experimental data
  - Predicts drainage transition: regime of complete depletion of trace component from bulk
    - verified in direct simulations
  - Corroborates *ex vivo* experimental data ➔ There is a *biomechanical* role for drugs in affecting leukocyte dynamics in blood

Ongoing work…

- More detailed experiments, especially re: parameter dependence
  - E.g. perfect drainage is not seen in expts. with platelets (e.g. Shaqfeh group)
- Extensions of theory and simulations: shape effects, finite concentration, RBC aggregation, adhesion to surfaces
- Complex geometries: connections to Zweifach-Fung effect, separation methods
- Time-dependent flows – e.g. LAOS
- Physiological relevance e.g. for sickle cell disease

Surfactant micelles

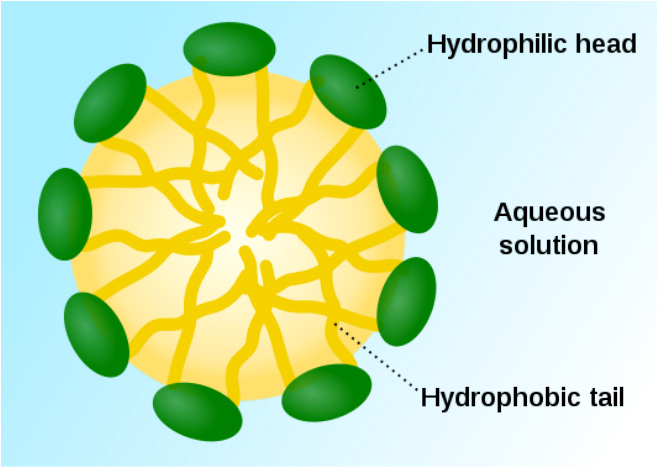

www.commons.wikimedia.org/wiki/File%3AMicelle_scheme-en.svg

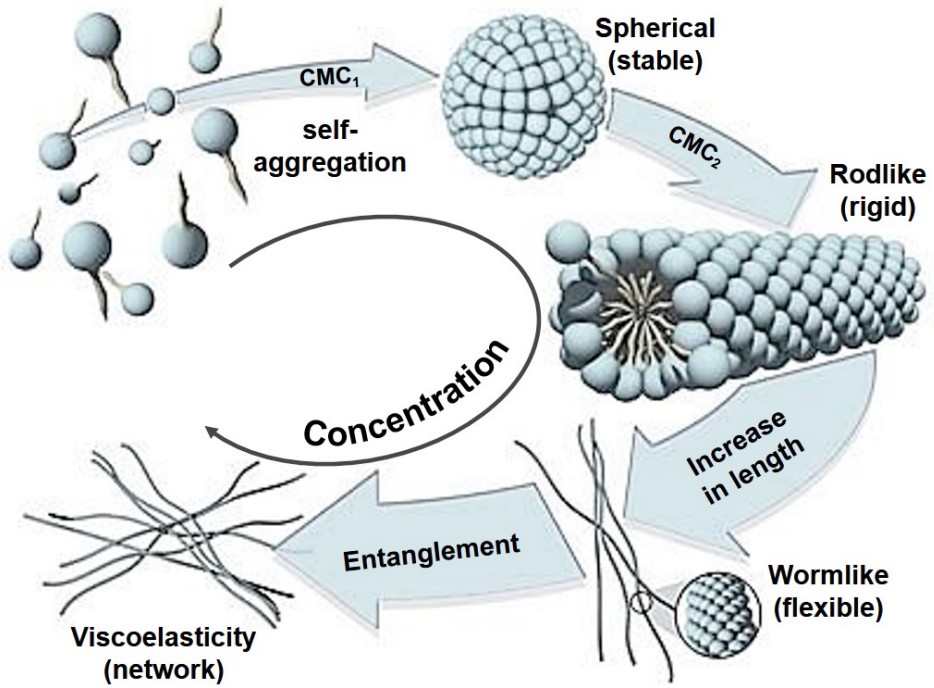

www.ethz.ch/ilw/vt/research/projects/vivianel

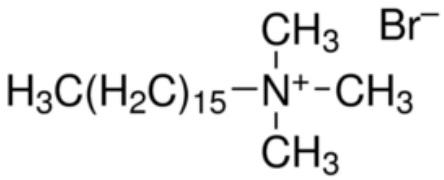

cetyltrimethylammonium bromide (CTAB)

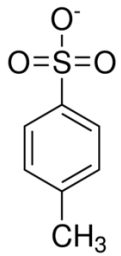

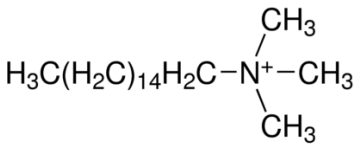

cetyltrimethylammonium p-toluenesulfonate (CTAT)

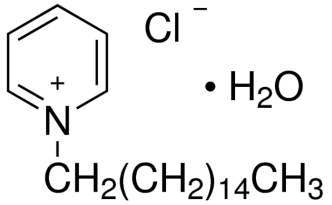

cetylpyridinium chloride (CPyC

Surfactant solutions: applications and phenomena

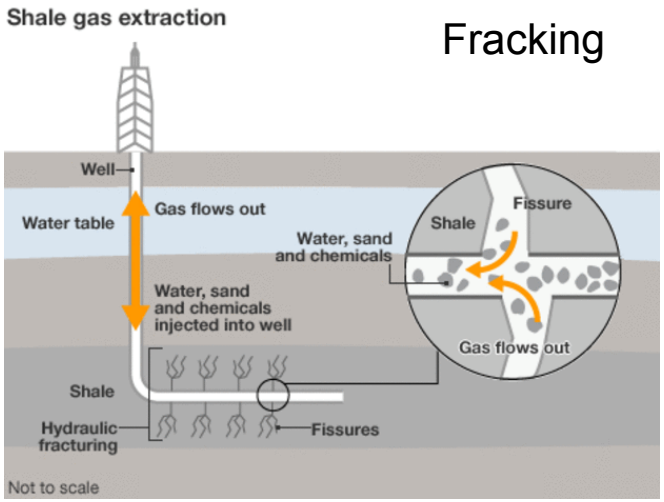

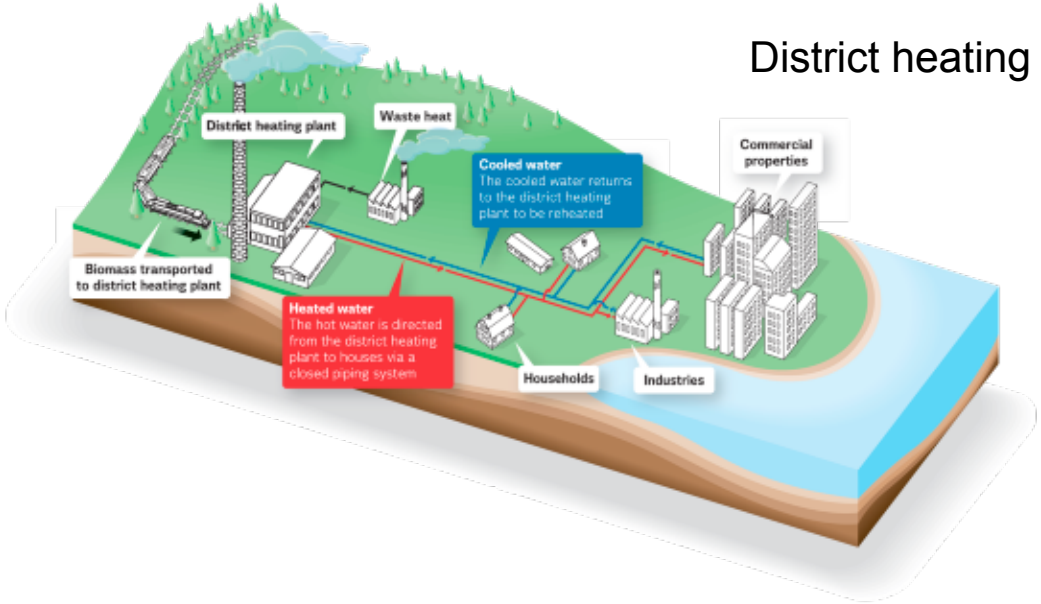

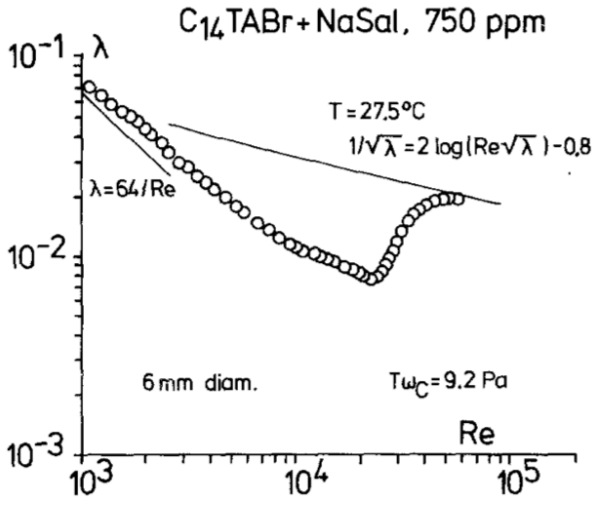

Ohlendorf et al, Rheol. Acta 25 (1986) 468

- Shear-thinning/thickening, flow-induced structure (FIS), shear-banding, etc.
- Turbulent drag reduction
- To study flow problems, we need a tractable constitutive model — like FENE-P for dilute polymer solutions

Flow induced structures (FIS)

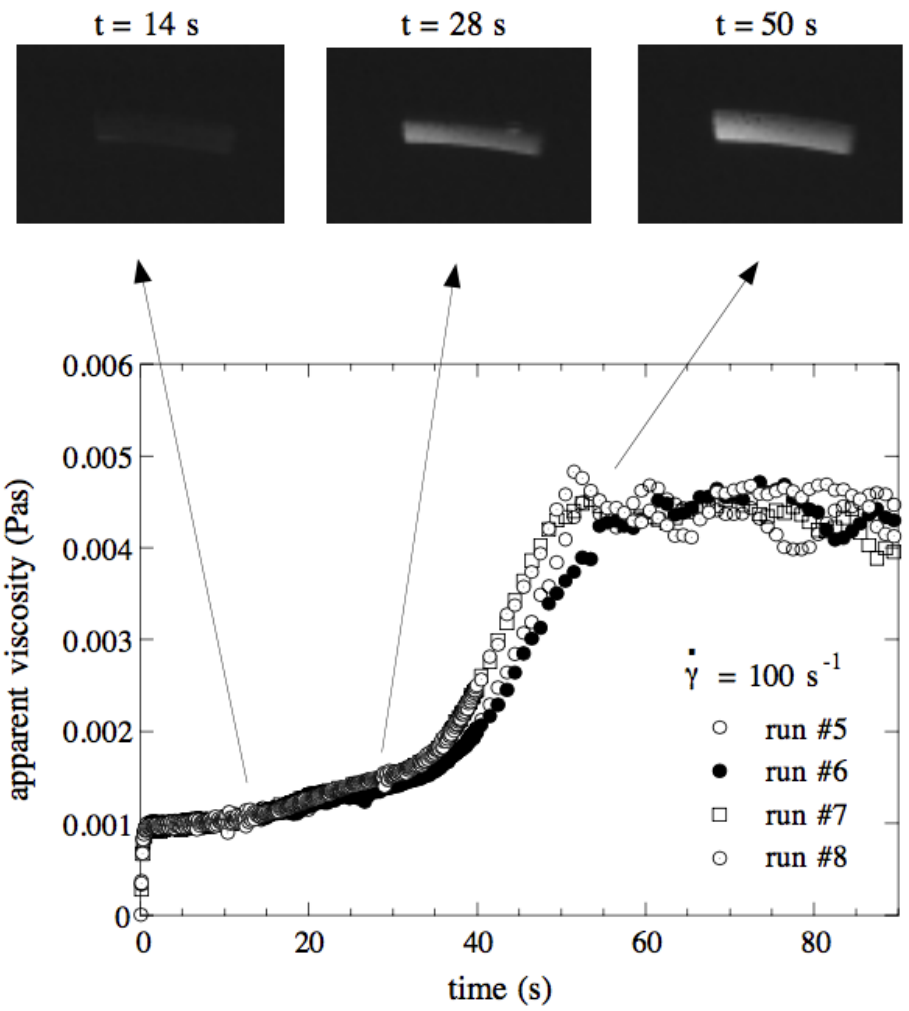

Berret et al, Eur. Phys. J. E 2 (2000) 343

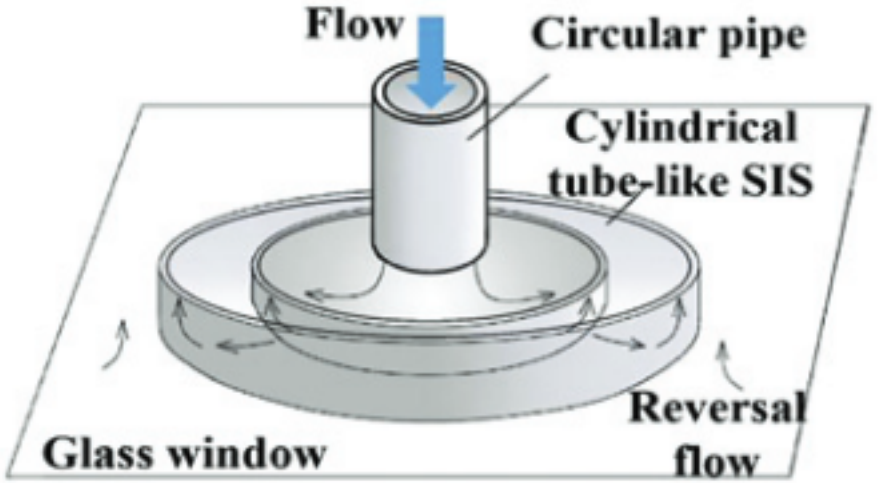

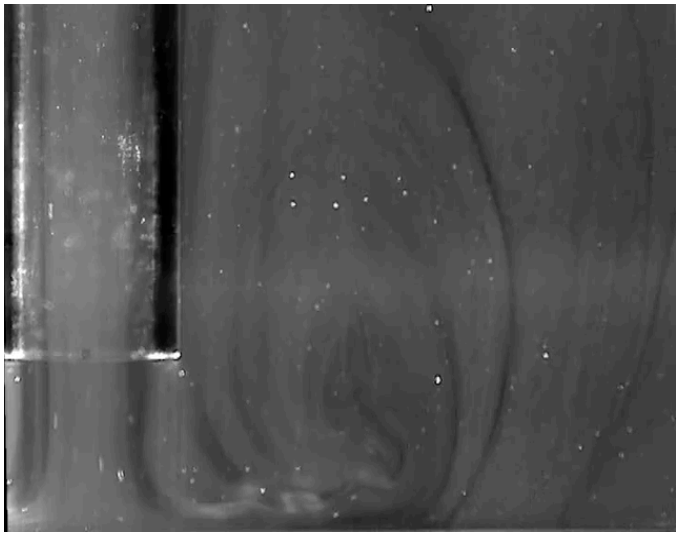

Tuan et al, J Rheol. 61 (2017) 83

Reentrant/discontinuous behavior

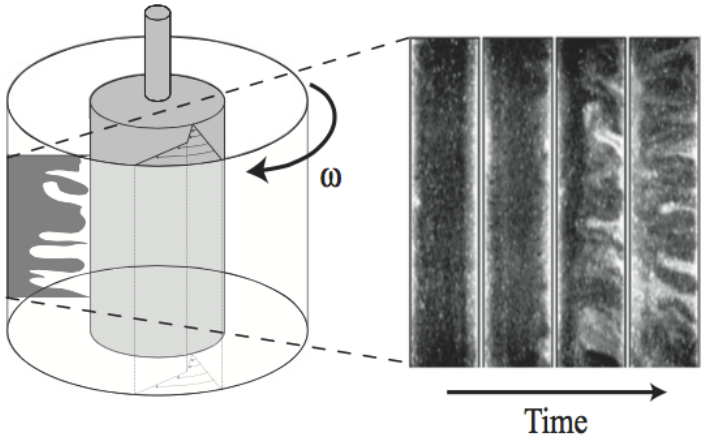

Liu & Pine, Phys. Rev. Lett. 77 (1996) 2121

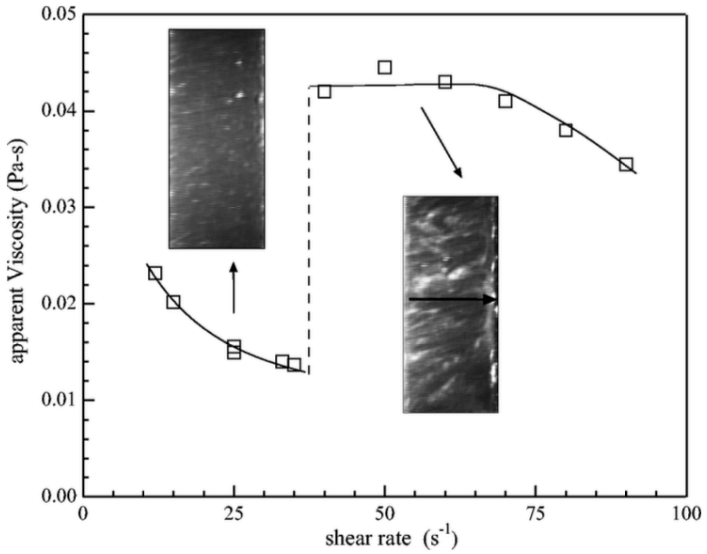

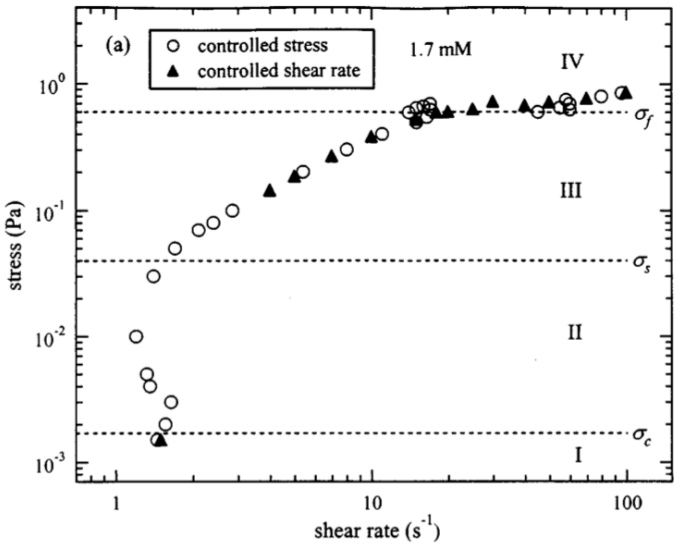

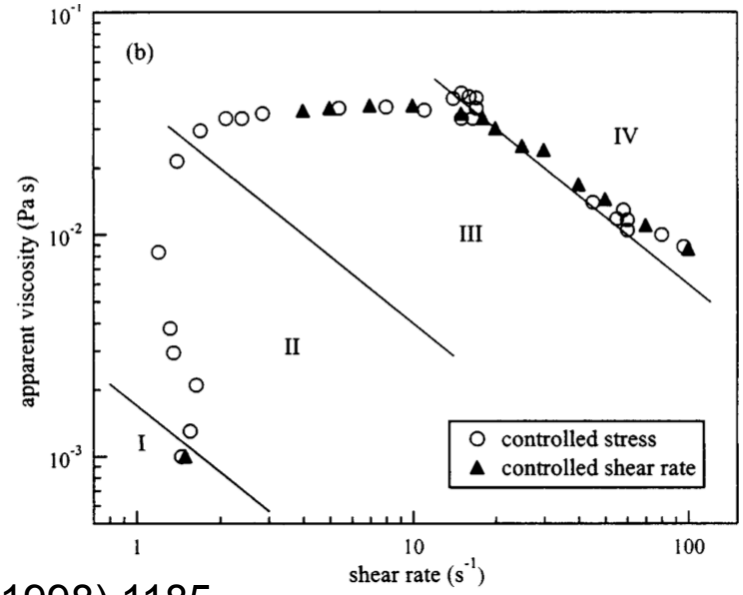

Hu et al, J. Rheol. 42 (1998) 1185

Shear banding vs. vorticity banding

Multiple shear rates for same shear stress

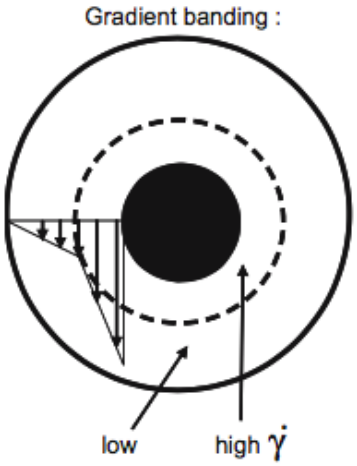

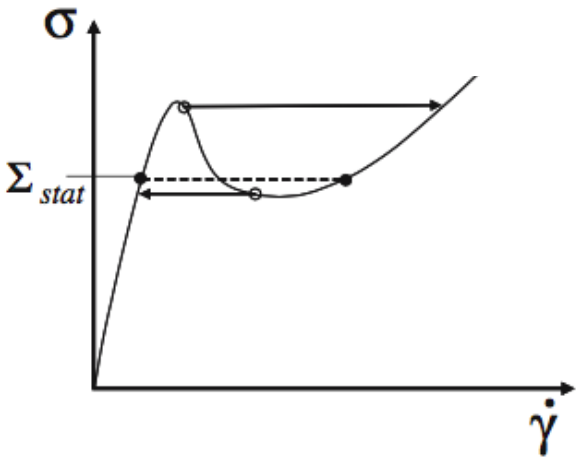

Vorticity banding :

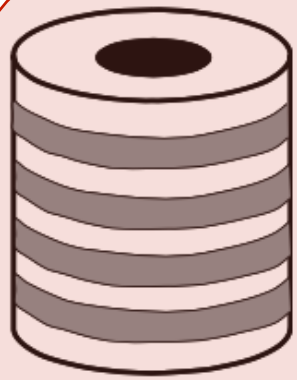

Multiple shear stresses for same shear rate

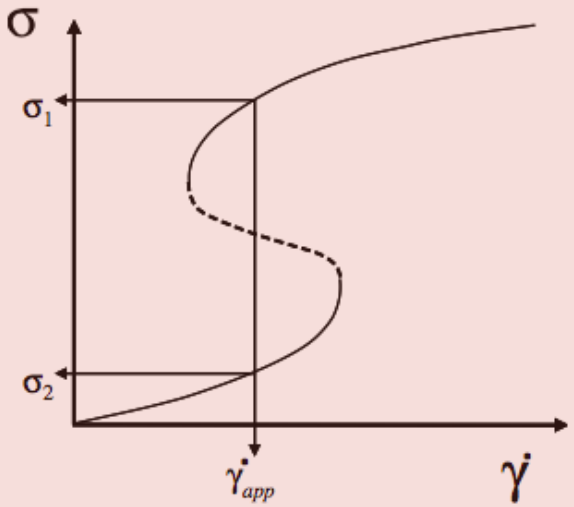

Dhont and Briels, Rheol. Acta 47: 257, 2008.

Mechanism for FIS formation (Cates & Turner)

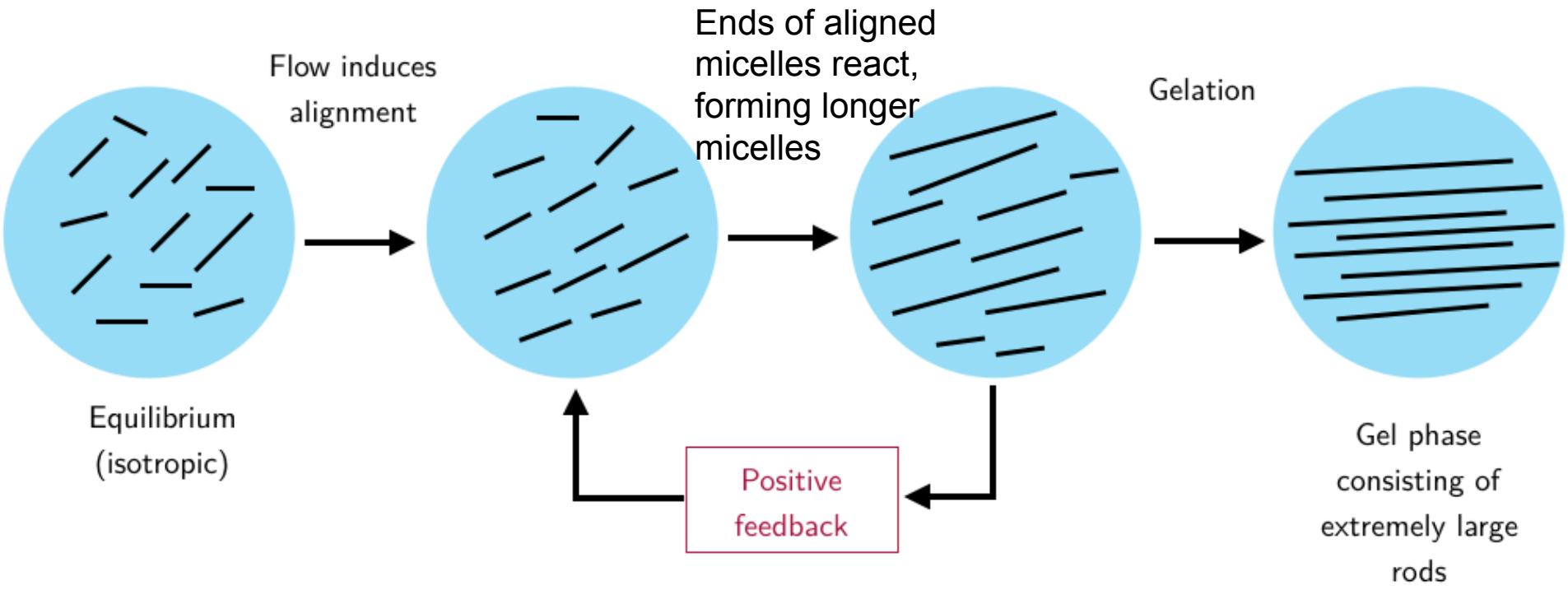

- Gelation appears due to divergence of the average rod length at a critical deformation rate
- Does not provide an expression for the evolution of stress ← **Our aim here**

Cates & Turner, Europhys. Lett. 11 (1990) 681, Turner & Cates, J. Phys.:Condens. Matter 4 (1992) 3719

“Reactive rod model” (RRM): setup

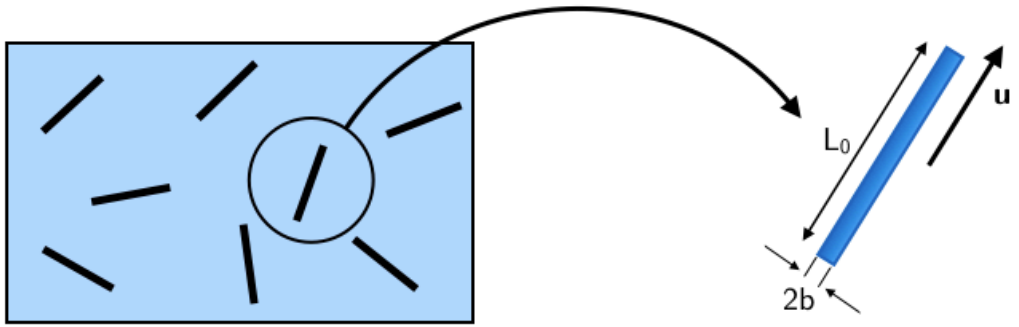

Rotational diffusivity: $D_{r,0} = \frac{3k_BT}{\pi\eta_s L_0^3} \ln\left(\frac{L_0}{2b}\right)$

Rotational diffusivity for rod length L: $D_r = \frac{D_{r,0}}{L^{*3}}\left(\frac{\ln L^* + m}{m}\right)$ where $m = \ln\left[L_0/(2b)\right]$, $L^* = L/L_0$

Orientation tensor: $\mathbf{S} = \langle \mathbf{uu} \rangle$ and $\hat{\mathbf{S}} = \mathbf{S} - \frac{1}{3}\mathbf{I}$ (traceless)

Scalar orientation parameter: $\hat{S} = \sqrt{\frac{3}{2}\left(\hat{\mathbf{S}} : \hat{\mathbf{S}}\right)}$ = 0 (isotropic); 1 (fully aligned)

$$Pe = \begin{cases} \dot{\gamma}/D_{r,0} & \text{for shear flow} \\ \dot{\varepsilon}/D_{r,0} & \text{for extensional flow} \end{cases}$$

Nondimensionalization: $t^* = tD_{r,0}$

S and *L* are the degrees of freedom of the RRM

Dutta & Graham, JNNFM to appear, 2017.

Reactive rod model: evolution of *L*

Assume narrow length distribution → only keep track of one representative length *L (not necessarily a good assumption)*

Evolution equation for L: $$\frac{dL^*}{dt^*} = R_a + R_s$$

Alignment-induced growth: $$R_a = k\hat{S}$$

Spontaneous growth and breakage: $$R_s = \frac{\lambda}{1 - \left(\frac{L^*}{L^*_{\max}}\right)^2}(1 - L^*)$$

Hydrodynamic tension limits R_s: $$L^*_{\max} = \alpha + \frac{\beta}{Pe}$$

Surfactant conservation → $$nL = n_0 L_0$$

Reactive rod model: orientation & stress

Time evolution of the orientation tensor $\mathbf{S} = \langle \mathbf{uu} \rangle$

$$\frac{d\mathbf{S}}{dt} = -6D_r \left(\mathbf{S} - \frac{1}{3}\mathbf{I} \right) + \mathbf{K} \cdot \mathbf{S} + \mathbf{S} \cdot \mathbf{K}^{\mathsf{T}} - 2\mathbf{K} : \langle \mathbf{uuuu} \rangle$$

$$\mathbf{K} = \nabla \mathbf{v}^{\mathsf{T}}, \mathbf{D} = \frac{1}{2}\left(\mathbf{K} + \mathbf{K}^{\mathsf{T}} \right)$$

Dhont-Briels closure:

$$\mathbf{K} : \langle \mathbf{uuuu} \rangle \approx \frac{1}{5}\left(\mathbf{D} \cdot \mathbf{S} + \mathbf{S} \cdot \mathbf{D} - \mathbf{S} \cdot \mathbf{S} \cdot \mathbf{D} - \mathbf{D} \cdot \mathbf{S} \cdot \mathbf{S} + 2\mathbf{S} \cdot \mathbf{D} \cdot \mathbf{S} + 3\mathbf{SS} : \mathbf{D} \right)$$

Exact at equilibrium and perfect alignment, satisfies all necessary invariances and symmetries

Stress tensor:

$$\boldsymbol{\tau} = 2\eta_s \mathbf{D} + 3nk_B T \left(\mathbf{S} - \frac{1}{3}\mathbf{I} \right) + \frac{nk_B T}{2D_r} \mathbf{K} : \langle \mathbf{uuuu} \rangle$$

- Coupling to L evolution is through D_r
- Linear viscoelastic behavior is same as simple rigid rods – coupling of L to S arises only at O(Pe^2)

Shear rheology

Shear stress

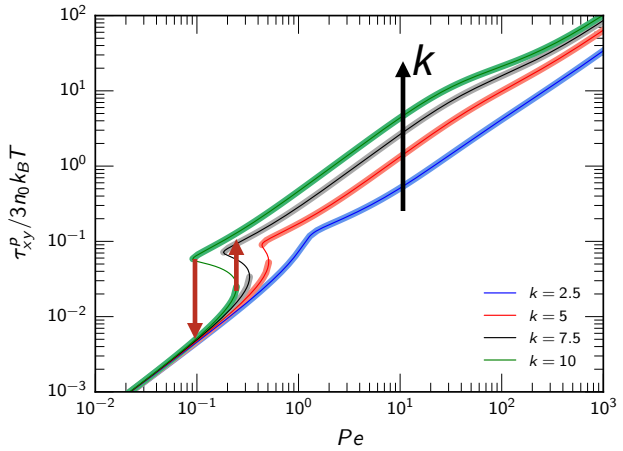

Rod length

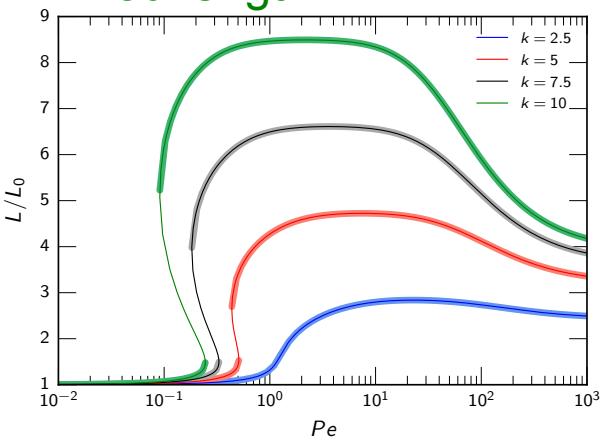

Viscosity

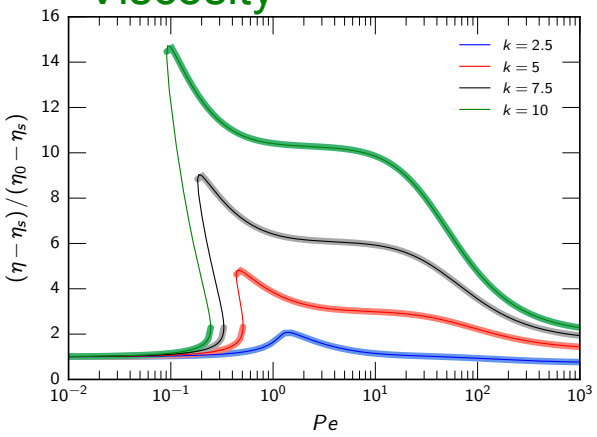

N_1

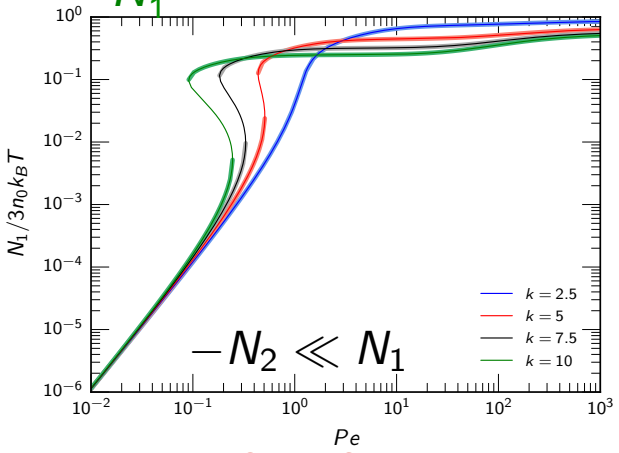

Stress and length are multivalued in a range of *Pe* for large enough growth rate constant *k*

Extensional rheology

Extensional stress

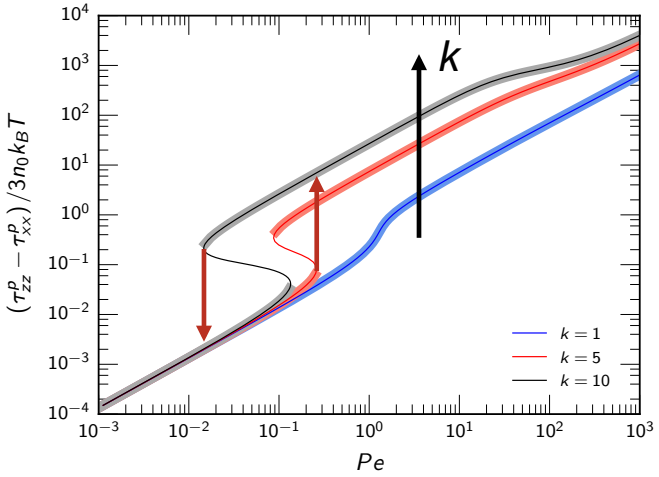

Rod length

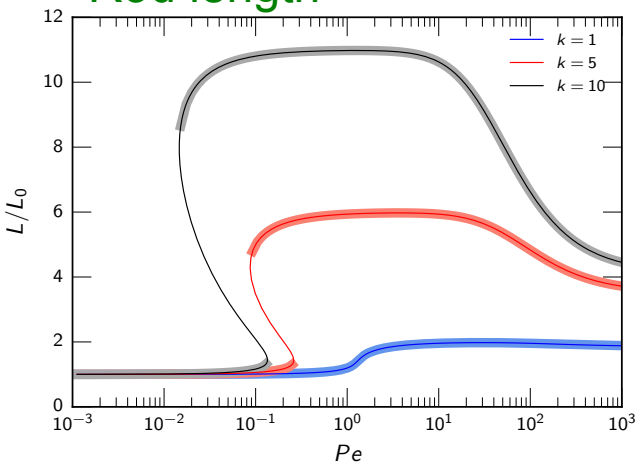

Extensional viscosity

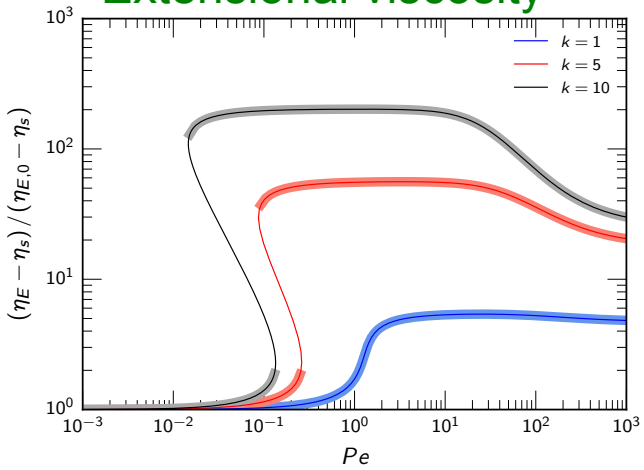

Stress and length are multivalued in a range of *Pe* for large enough growth rate constant

Multiplicity regimes in shear and uniaxial extension

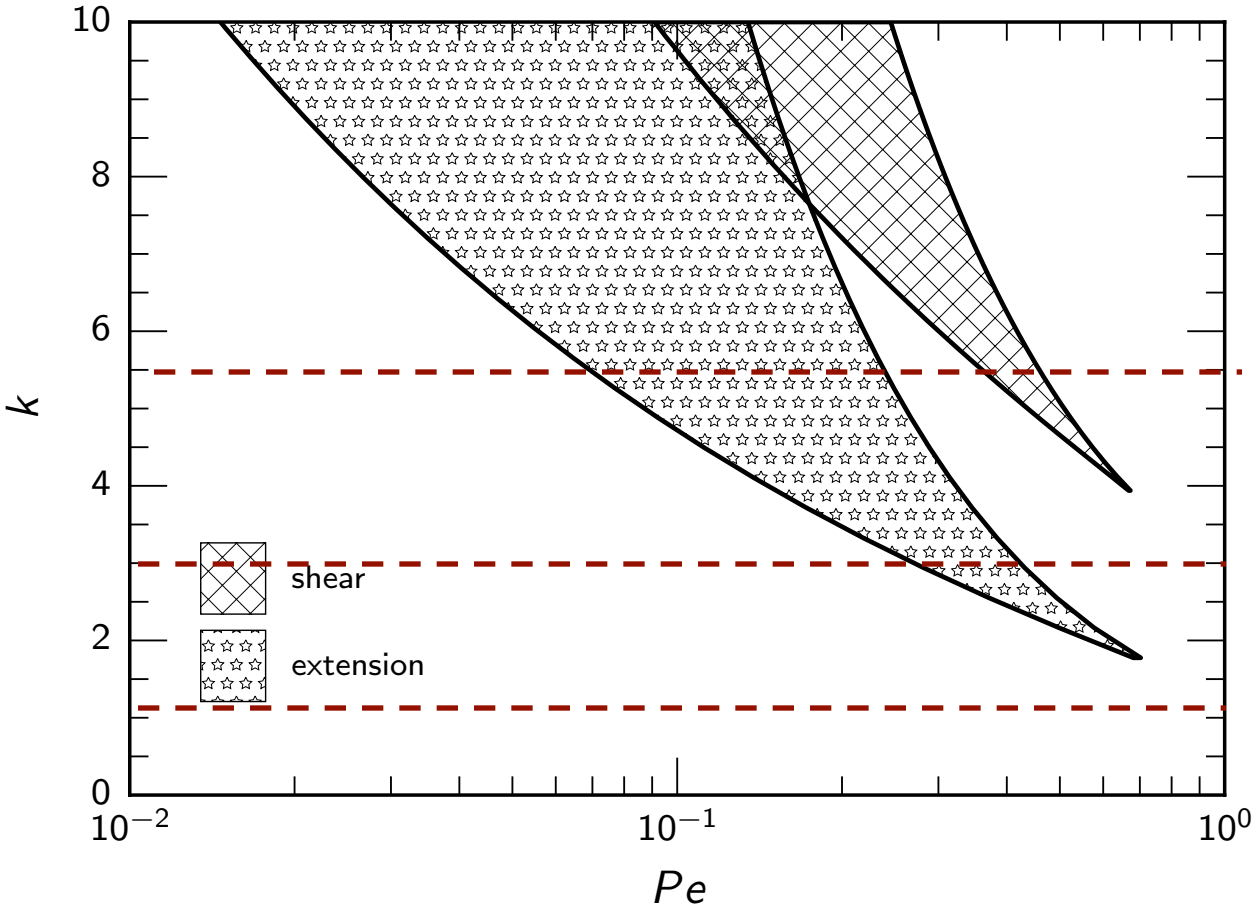

Multiplicity regimes

- Larger in extension than shear
- Starts at lower Pe in extension

Comparison with experiments

shear flow

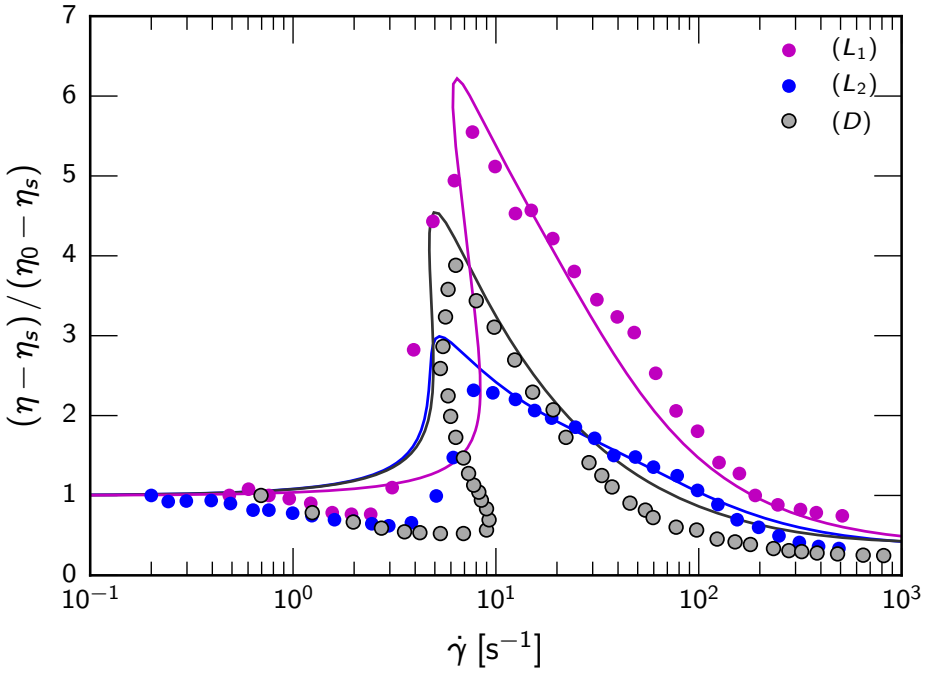

extensional flow

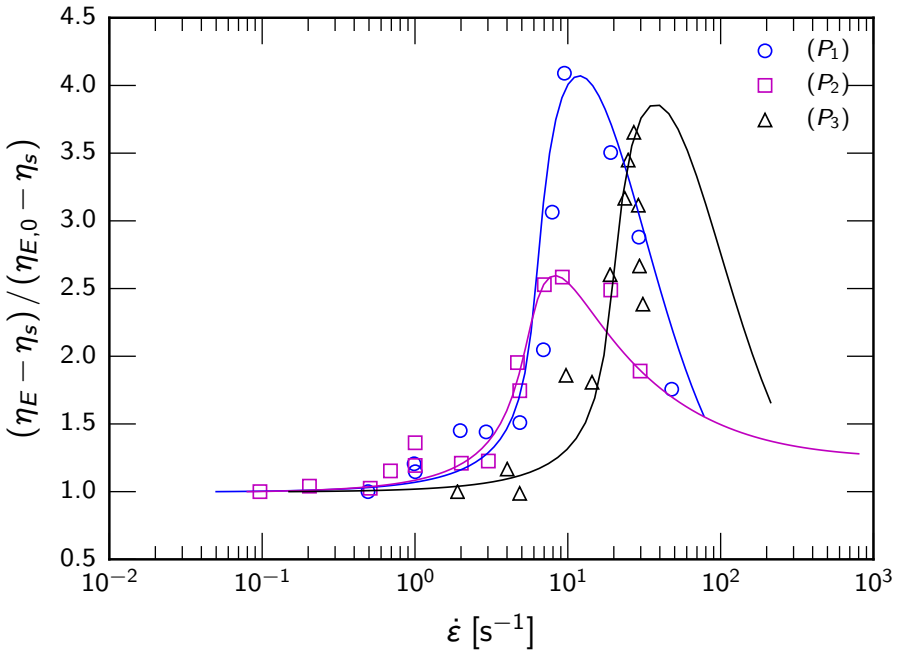

Model predictions (lines) show reasonable agreement with experiments

Liu & Pine, Phys. Rev. Lett. 77 (1996) 2121

Dehmoune et al, Rheol. Acta 46 (2007) 1121

Prudhomme & Warr, Langmiur 10 (1994) 3419

Conclusions

- RRM predicts shear (extension)-thickening in WMS with subsequent shear (extension)-thinning
- Predicts a multivalued stress at a given strain rate over a wide parameter ranges — associated with discontinuous shear thickening & FIS formation
- Model predictions are in reasonable agreement with experiments
- Computationally tractable: comparable to FENE-P

Future work/Open issues

- Model refinements
  - Better physical models for micelle growth/breakage
    - E.g. make breakage rate scale as chain tension $(nL)^{-1}\langle \mathbf{uu} \rangle : \boldsymbol{\tau}^p$
    - Incorporate branching to better model gel-like behavior
  - More comparisons with expt. (e.g. transients)
  - Is there a first-principles theory that can be reduced systematically to something like this?
- Fluid dynamics! Spatiotemporal evolution of FIS
  - Circular Couette: “interfacial instability” (Pine observations)
  - How does vorticity banding arise? (Is it related to previous point?)
  - Turbulence in surfactant solutions
  - Potentially interesting computational issues: intricate nonequilibrium “phase” interfaces

Thank you